Supporting Information

Discovery and Biosynthesis of Tetrachlorizine Reveals Enzymatic Benzylic Dehydrogenation via an *ortho*-Quinone Methide

Trevor N. Purdy, [†] Min Cheol Kim,[†] Reiko Cullum,[†] William Fenical,*[,†,‡,§]
Bradley S. Moore*[,†,§]

[†]Center for Marine Biotechnology and Biomedicine, Scripps Institution of Oceanography, [‡]Moores Comprehensive Cancer Center, [§]Skaggs School of Pharmacy and Pharmaceutical Sciences, University of California at San Diego, La Jolla, CA, 92093, United States

Table of Contents

1. Materials

All chemicals were purchased from Fisher Scientific, Alfa Aesar, or MilliporeSigma without further purification. All solvents were of HPLC grade or higher. Preparative flash column chromatography was carried out on a Teledyne ISCO CombiFlash® Rf+ Lumen™ system using diatomaceous earth for crude extract loading and silica gel 60 (EMD, 40-63μm) for the stationary phase. Semi-preparative HPLC purification was carried out using a Phenomenex Luna C18 column (5 μm, 250 × 10 mm) at a flow rate of 3.0 mL/min, coupled with a Shimadzu SCL-10A system and Shimadzu SPD-M10A UV/Vis detector (Shimadzu Corp., Kyoto, Japan). Preparative HPLC purification was achieved using a Phenomenex Luna C18 column (5 μm, 100 x 2.0 mm) at a flow rate of 10.0 mL/min, coupled with an Agilent Technologies system composed of a PrepStar pump, a ProStar 410 autosampler, and a ProStar UV detector (Agilent Technologies Inc., CA, USA). UV spectra were measured with a Beckman Coulter DU800 spectrophotometer with a path length of 1 cm, and IR spectra were acquired on a JASCO FTIR-4100 spectrometer. NMR spectroscopic data were obtained either on a 500 MHz JEOL NMR spectrometer with a 3.0 mm probe, a 600 MHz Bruker NMR spectrometer with a 1.7 mm cryoprobe, or a 500 MHz Varian NMR spectrometer with a 5 mm, ^{13}C optimized cold probe. The values of the chemical shifts are described in ppm and coupling constants are reported in Hz. NMR chemical sifts were referenced to the residual solvent peaks (d_H 2.50 and d_C 39.5 for DMSO-d_6; d_H 8.74, 7.58, and 7.21 and d_C 149.9, 135.5, and 123.5 for pyridine-d_5). High resolution LC-MS (HR-LC-MS) analysis was conducted on an Agilent 6530 Accurate-Mass Q-TOF MS (MassHunter software, Agilent) equipped with a dual electrospray ionization (ESI) source and an Agilent 1260 LC system (ChemStation software, Agilent) with a diode array detector. Q-TOF MS settings during the LC gradient were as follows: acquisition - mass range acquisition m/z 100 – 1700, MS scan rate 10/s, MS/MS scan rate 2/s, fixed collision energy 20 eV; source - gas temperature 300 °C, gas flow 11 L/min; nebulizer 35 psig, ion polarity negative; scan source parameters - VCap 3000, Fragmentor 100, Skimmer 65, OctopoleRFPeak 750.

Plasmid DNA was isolated from an overnight culture using the QIAprep Spin miniprep Kit (Qiagen, Hilden, Germany) according to the manufacturer's protocol. DNA clean-up after PCR or agarose gel electrophoresis was performed with QIAquick PCR & Gel Cleanup Kit according to the manufacturer's protocol. DNA sequencing was carried out by the Genewiz Sequencing Facility in San Diego, CA.

Sonication of *E. coli* cells was performed using a 6 mm tip (Qsonica, CT, USA). Protein purification was performed on an ÄKTApurifier instrument (GE Healthcare, IL, USA) with the modules Box-900, UPC-900, R-900 and Frac-900 with all buffers filtered through a nylon membrane 0.2 μm GDWP (Merck, NJ, USA) prior to use. FPLC data was analyzed with UNICORN 5.31 (Built 743) software. All proteins were purified by Ni^{2+} affinity chromatography using a 5 mL HisTrap HP (GE Healthcare) column. Proteins were concentrated using Amicon Ultra filters with 50 kDa MWCO (MilliporeSigma). Buffer exchange was performed by size exclusion chromatography using a HiLoad 16 × 60 cm Superdex 75 prep grade column (GE Healthcare).

2. Bacterial Strains and Growth Conditions

Cultivation and Purification of tetrachlorizine (1) and dihydrotetrachlorizine (2)

Actinomycete sp. AJS-327 was previously isolated from a sponge fragment that washed ashore in La Jolla, CA.[1] Actinomycete sp. AJS-327 was cultured in 500 mL of a seawater-based A1 medium (10 g of starch, 4 g of yeast, 2 g of peptone, 300 mL of deionized water, and 700 mL of seawater), shaking at 180 rpm and 27 °C. After 4 days of cultivation, the culture medium was used to inoculate 20 × 2.8 L Fernbach flasks each containing 1 L of seawater-based A1 medium and shaken at 180 rpm and 27 °C. After an additional 7 days of cultivation, 20 g of Amberlite XAD-7 resin was added to each flask and shaking was continued at 180 rpm for 4 hours. The resin was collected by filtration through cheesecloth and washed with deionized water. The washed resin was extracted with acetone, and the solvent was removed under vacuum. The remaining solution was then extracted with ethyl acetate, and the ethyl acetate layer was collected and evaporated under reduced pressure to yield 3.8 g of organic extract.

The crude extract was fractionated using Lichroprep RP-18 (40-63 μm, Merck) and a step gradient elution with H_2O and CH_3OH (20%, 40%, 60%, 80%, and 100%; each 200 mL) to give five subfractions. The 100% CH_3OH fraction (1.5 g) was subjected to re-fractionated by silica vacuum flash chromatography using a step gradient solvent system with CH_2Cl_2 and CH_3OH (0%, 2%, 3%, 5%, 10%, 50%, and 100% CH_3OH; each 100 mL) to afford seven fractions. Fractions 2 (60 mg) and 3 (350 mg) were subjected to reversed-phase preparative HPLC (UV detection at 350 nm) using gradient elution from 10% to 100% aqueous CH_3CN in 0.02% TFA over 60 min to obtain compounds **1** (t_R 47.9 min) and **2** (t_R 46.8 min). Both compounds were further purified by reversed-phase semi-preparative HPLC (UV detection at 350 nm) with an CH_3CN/H_2O (in 0.02% TFA) gradient elution system from 60% to 100% for 30 min, which resulted in the isolation of **1** (6.5 mg) and **2** (2.8 mg).

Tetrachlorizine (1):

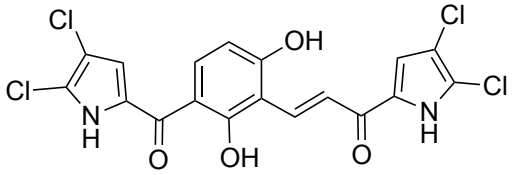

Dark orange gum; UV (CH_3OH) λ_{max} (log ε) 354 (3.99) nm; IR (ZnSe) ν_{max} 3221, 1685, 1585, 1414, 1262, 1208, 1138 cm^{-1}; ^1H and ^{13}C NMR data, see Tables S2-3; HR-ESI-TOFMS: m/z = 456.9317 $[M-H]^-$ (calcd. for $C_{18}H_9{}^{35}Cl_4N_2O_4$, 456.9301).

Dihydrotetrachlorizine (2):

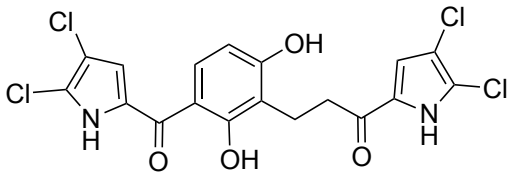

Yellow gum; UV (CH_3OH) λ_{max} (log ε) 227 sh (3.59), 244 (3.50), 297 (3.80), 350 (3.83) nm; IR (ZnSe) ν_{max} 3218, 1601, 1563, 1490, 1420, 1301, 1251, 1174, 1136, 1082, 1025 cm^{-1}; ^1H and ^{13}C NMR data, see Tables S2 and S4; HR-ESI-TOFMS: *m/z* = 458.9496 $[M-H]^-$ (calcd. for $C_{18}H_{11}{}^{35}Cl_4N_2O_4$, 458.9472).

Purification of prechlorizidine (4)

Heterologous expression of the *clz* gene cluster and characterization of prechlorizidine has been previously reported.[2] Cultivation of the deletion mutant *Streptomyces coelicolor* M512_4B11Δclz9 and isolation of prechlorizidine (**4**) was performed following a modified procedure; briefly, colonies of *S. coelicolor* M512_4B11Δclz9 were inoculated in 2 × 250 mL flasks containing 50 mL of TSB media supplemented with kanamycin (50 mg/mL^{-1}) and nalidixic acid (25 mg/mL) for 5 days and shaken at 180 rpm and 30 °C. The cultures were then transferred to 2.8 mL Fernbach flasks containing 1 L of R5 media supplemented with kanamycin (50 mg/mL) and shaken at 180 rpm and 30 °C. After an additional 7 days of cultivation, 800 mL of EtOAc was added to each flask and shaken for 1 additional hour. The cultures were combined and centrifuged. The supernatant was extracted, and the organic layer was separated and dried over $MgSO_4$. The solvent was then evaporated under reduced pressure and the crude extract was loaded onto diatomaceous earth. The crude extract was eluted onto silica for flash column purification using a gradient from 0–20% EtOAc in hexanes over 20 minutes. The solvent was evaporated under reduced pressure, which resulted in the isolation of **4** (22.4 mg).

3. Protein Expression, Purification, and *In Vitro* Assay Conditions

Cloning and Expression of Clz9 and Tcz9

Cloning and expression of Clz9 has been previously reported.[2] Actinomycete sp. AJS-327 gDNA was isolated following standard procedures and concentrated using an isopropanol precipitation procedure.[3,4] The gene coding for Tcz9 was amplified from gDNA using PrimeSTAR Max DNA polymerase (Takara Bio Inc., Kyoto, Japan) and oligonucleotides Tcz9_MBP_F (CTGTACTTCCAATCCG-GATCCATGGCCACCCCATCCGCATTC) and Tcz9_MBP_R (GGTGGTGGTGGTGCTCGAG-TCAGTCCAGCGGTCCGTCGA). The resulting 1.5-kb PCR product was cloned into a PCR amplified pET28a_MBP vector using oligonucleotides Tcz9_MBP_F and Tcz9_MBP_R by Gibson Assembly using HiFi DNA Assembly Master Mix (New England Biosciences, MA, USA). The resulting construct, Tcz9_MBP, was isolated from *E. coli* DH10B, verified by DNA sequencing and then transformed into *E.*

coli BL21 (DE3) cells for protein expression. Expression of Tcz9 was started by inoculating an overnight culture at 200 rpm and 37 °C with a single colony of *E. coli* BL21 (DE3) harboring Tcz9_MBP, in Luria-Bertani (LB) broth supplemented with kanamycin (50 μg/mL) and chloramphenicol (12.5 μg/mL). The cultures were then transferred to 2.8 mL Fernbach flasks containing 1 L of terrific broth (TB) media supplemented with kanamycin (50 μg/ml), chloramphenicol (12.5 μg/mL), and riboflavin (~100 mg/L). After incubation at 200 rpm and 30 °C until an OD_{600} = 0.8 was reached (approximately 4 hours), the temperature was lowered to 18 °C and protein expression was induced by the addition of IPTG (0.1 mM final concentration). The culture was incubated at 200 rpm and 18 °C for 20 hours until stopped by harvesting the cells via centrifugation (7,500g, 4 °C, 30 min). The cell pellet was stored at –80 °C.

Purification of Clz9 and Tcz9

The purification of Clz9 and Tcz9 was performed following a modified procedure that was previously reported.[2] Frozen cell pellets were thawed and then suspended in lysis buffer (2 mL/g cells, 20 mM Tris-HCl pH 8.0, 500 mM NaCl, 10% glycerol). The cells were then sonicated at 40% amplitude for 20 cycles of 15 seconds on and 45 seconds off while remaining chilled on ice. The lysate was recovered by centrifugation (10,000g, 4 °C, 30 min) and purified by Ni^{2+} affinity chromatography over a 30 minute gradient from 10–100% elution buffer (20 mM Tris, 200 mM NaCl, 30 mM imidazole, pH 8.0) in wash buffer (20 mM Tris, 200 mM NaCl, 250 mM imidazole, pH 8.0). Eluting fractions were evaluated for purity by SDS-PAGE, and pure fractions were collected and concentrated using a 50 kDa MWCO spin filter. The protein was further purified by size exclusion chromatography preequilibrated with a 100 mM potassium phosphate buffer (5% glycerol, pH 7.5). Clz9 and Tcz9 were concentrated to approximately 20 mg/mL prior to aliquoting and storage at –80 °C.

General Procedure for *in vitro* Assays with Clz9 and Tcz9

The *in vitro* assays were performed following a modified procedure that was previously reported.[2] A solution containing **2** or **4** (1 mM) in DMSO was suspended in potassium phosphate buffer (5 mL, pH 7.5, with 0.2 mg/mL catalase and 10% DMSO). The reaction was initiated with addition of Clz9 or Tcz9 (50 μM final concentration) and incubated for 12 hours at 37 °C.

5,6-dichloro-3-(3-(4,5-dichloro-1*H*-pyrrole-2-carbonyl)-2,6-dihydroxyphenyl)-2,3-dihydro-1*H*-pyrrolizin-1-one (8):

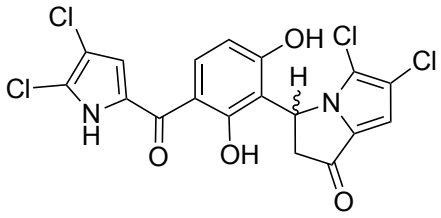

Following incubation for 12 hours, the reaction was transferred to a 15 mL falcon tube and extracted with three times with EtOAc. The organic layer was washed with brine and dried using $MgSO_4$. The crude mixture was then concentrated and loaded onto celite for silica flash chromatography using a gradient from 0 – 20% CH_3OH in DCM. The solvent was evaporated under reduced pressure, which resulted in the isolation of 4 (300 µg).

UV (CH_3OH) λ_{max} 227, 244, 297, 354 nm; ^1H and ^{13}C NMR data, see Tables S5-6; HR-ESI-TOFMS: *m/z* = 456.9333 $[M-H]^-$ (calcd. for $C_{18}H_9{}^{35}Cl_4N_2O_4$, 456.9317).

(*E*)- and (*Z*)-2,3-dichloro-7-(5,6-dichloro-3*H*-pyrrolizin-3-ylidene)-8-hydroxy-5*H*-pyrrolo[2,1-*a*]isoindole-5,6(7*H*)-dione (9) and (10) (unable to unambiguously differentiate isomers):

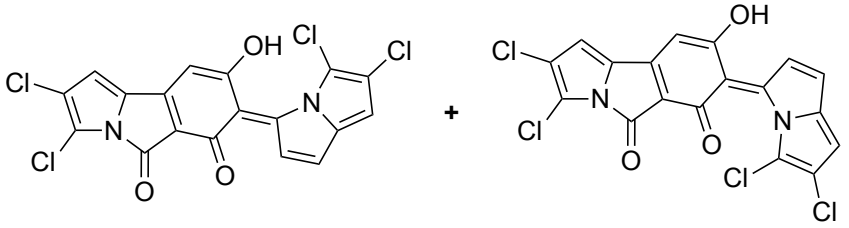

Over the course of the reaction, a red solid slowly precipitated out of solution. This precipitate was vacuum filtered over Celite and rinsed with three times with water to remove residual DMSO. The precipitate was resuspended in CH_3OH and loaded onto Celite for silica flash chromatography using a gradient from 0 – 8%, then flushed with 20% CH_3OH in DCM. The solvent was evaporated under reduced pressure, which resulted in the isolation of **9** and **10** (100 µg and 800 µg).

The desired product strongly binds to $MgSO_4$; thus, certain drying agents should be avoided when removing water from organic solvent solutions containing this product. Compounds **9** and **10** have very limited solubility in common organic solvents, including EtOAc, DCM, MeCN, and acetone.

UV (CH_3OH) λ_{max} 246, 280, 370, 426, 452, 481, 510, 535 nm; ^1H data, see Table S7; HR-ESI-TOFMS: *m/z* = 436.9058 and 436.9065 $[M-H]^-$ (calcd. for $C_{18}H_5{}^{35}Cl_4N_2O_3$, 436.9055).

(*E*)-2,3-dichloro-7-(3-(4,5-dichloro-1*H*-pyrrol-2-yl)-3-oxoprop-1-en-1-yl)-6,8-dihydroxy-5*H*-pyrrolo[2,1-*a*]isoindol-5-one (13):

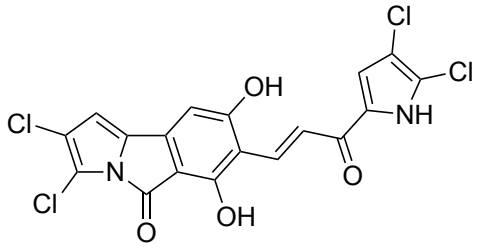

Over the course of 24 – 48 hours, isomers **9** and **10** slowly converged to the same yellow product (**13**) while dissolved in DMSO-d_6. The product was further characterized by NMR. ^{1}H and ^{13}C chemical shifts at C-13, C-14, and C15 closely matched the corresponding atoms in **1** to help confirm the absolute structure.

UV (CH_3OH) λ_{max} 224, 263, 354, 420 nm; ^{1}H and ^{13}C NMR data, see Tables S8-9; HR-ESI-TOFMS: *m/z* = 454.9171 $[M-H]^-$ (calcd. for $C_{18}H_7{}^{35}Cl_4N_2O_4$, 454.9160).

4. Supplementary Tables

Table S1. Putative functions of the genes in the BGC associated with **2** and sequence comparisons with *clz* genes[2] or closest homologues.

Gene	Size (a.a.)	Predicted Function	*clz*[2] or closest homolog (% Protein Identity)	GenBank Accession Number
tcz1	146	MarR family transcriptional regulator	*S. cacaoi* (84)	WP_171394890.1
tcz2	131	Putative sterol carrier protein	*clz2* (62)	WP_158692259.1
tcz3	262	Enoyl-ACP reductase	*clz3* (73)	WP_027747159.1
tcz4	392	2-alkenoyl-CoA carboxylase/reductase	*clz4* (78)	WP_106965699.1
tcz5	448	FAD-dependent halogenase	*clz5* (81)	WP_027747161.1
tcz6	3015	Type I PKS	*clz6* (54)	WP_051262040.1
tcz7	1515	Type I PKS	*clz7* (57)	WP_051262041.1
tcz8	560	FAD-dependent halogenase (inactive)	*clz8* (46)	WP_027747162.1
tcz9	477	FAD-dependent oxidoreductase (BBE-like)	*clz9* (53)	WP_051262042.1
tcz10	91	ACP	*clz10* (67)	WP_027747163.1
tcz11	436	KS type II	*clz11* (65)	WP_051262043.1
tcz12	246	Transporter ATP-binding protein	*S. varsoviensis* (77)	WP_030877486.1
tcz13	257	ABC transporter permease	*S. varsoviensis* (84)	WP_030877482.1
tcz14	210	TetR family regulator	*clz12* (60)	WP_078512405.1
tcz15	225	LuxR family regulator	*clz13* (59)	WP_158692260.1
tcz16	490	Adenyltransferase	*clz14* (69)	WP_027747166.1
tcz17	378	Acyl-CoA dehydrogenase	*clz15* (70)	WP_027747167.1
tcz18	451	Na^+/H^+ exchanger	*clz16* (66)	WP_051262045.1
tcz19	248	PPTase	*clz17* (51)	WP_051262046.1
tcz20	97	ACP	*clz18* (62)	WP_027747168.1
tcz21	263	Thioesterase	*clz19* (58)	WP_051262049.1
tcz22	335	Hypothetical Protein	*S. coeruleorubidus* (57)	WP_150481289.1

Abbreviations: ACP (acyl carrier protein); CoA (coenzyme A); FAD (flavin adenine dinucleotide); PKS (polyketide synthase); BBE-like (berberine bridge enzyme-like); KS (ketoacyl synthase); ATP (adenosine triphosphate); PPTase (phosphopantetheinyl transferase)

Table S2. ^{1}H and ^{13}C NMR spectroscopic data for **1** and **2**.

	1 (DMSO-d_6)		**2** (DMSO-d_6)		**2** (pyridine-d_5)	
position	δ_C, type[a]	δ_H, mult (J in Hz)[b]	δ_C, type[a]	δ_H, mult (J in Hz)[b]	δ_C, type[a]	δ_H, mult (J in Hz)[b]
2	120.4, C[e]		119.7, C[e]		120.5, C[e]	
3	110.1, C[e]		109.8, C[e]		110.9, C[e]	
4	117.7, CH	7.20, d (2.8)	117.1, CH	7.10, d (2.9)	117.9, CH	7.21, m[c,d]
5	127.1, C		127.4, C		128.9, C	
6	184.1, C		184.2, C		185.3, C	
7	110.9, C		111.0, C		112.3, C	
8	164.9, C		162.5, C		164.0, C	
9	109.7, C		114.0, C		115.6, C	
10	164.4, C		162.3, C		163.8, C	
11	108.2, CH	6.65, d (9.0)	107.8, CH	6.54, d (9.0)	108.2, CH	6.82, d (8.9)
12	134.8, CH	7.99, d (9.0)	131.0, CH	7.79, d (9.0)	131.5, CH	8.01, d (8.9)
13	132.6, CH	8.07, d (15.8)	18.2, CH_2	2.86, m[c]	19.5, CH_2	3.63, m
14	123.2, CH	7.85, d (15.8)	36.2, CH_2	2.86, m[c]	37.4, CH_2	3.37, m
15	178.1, C		188.6, C		189.5, C	
16	131.0, C		129.3, C		130.6, C	
17	115.0, CH	7.18, d (2.3)	115.4, CH	7.13, d (2.7)	116.0, CH	7.22, s
18	109.6, C[f]		109.2, C[f]		110.3, C[f]	
19	120.0, C[f]		119.4, C[f]		120.1, C[f]	
1-NH		13.36, br d (2.8)		13.05, br s		
8-OH		13.70, br s		13.25, br s		
10-OH		11.79, br s		10.76, br s		
20-NH		13.24, br d (2.3)		12.70, br s		

[a]125 MHz. [b]500 MHz. [c]Overlapping signals. [d]confirmed by HSQC. [e,f]Signals maay be switched.

Table S3. COSY, HMBC, and ROESY NMR data for **1** (500 MHz, DMSO-d_6).

1 (DMSO-d_6)				
position	δ_H/δ_C	COSY	HMBC	ROESY
4	7.20/117.7	H-1-NH	C-2, C-5	H-12
11	6.65/108.2	H-12	C-7, C-9	
12	7.99/134.8	H-11	C-6, C-8, C-10	H-4
13	8.07/132.6	H-14	C-10, C-15	
14	7.85/123.2	H-13	C-9, C-15	H-17
17	7.18/115.0	H-20-NH	C-16, C-19	H-14
1-NH	13.36/-	H-4	C-3	
8-OH	13.70/-		C-7, C-8, C-9	
10-OH	11.79/-		C-9, C-10	
20-NH	13.24/-	H-17	C-19	

Table S4. COSY, HMBC, and ROESY NMR data for **2** (500 MHz, DMSO-d_6 and pyridine-d_5).

2 (DMSO-d_6)				**2** (Pyridine-d_5)			
position	δ_H/δ_C	COSY	HMBC	δ_H/δ_C	COSY	HMBC	ROESY
4	7.10/117.1	H-1-NH	C-2, C-5	7.21/117.9		C-2, C-5	H-12
11	6.54/107.8	H-12	C-7, C-9	6.82/108.2	H-12	C-7, C-9	
12	7.79/131.0	H-11	C-6, C-8, C-10	8.01/131.5	H-11	C-6, C-8, C10	H-4
13	2.86/18.2	H-14	C-10, C-15	3.63/19.5	H-14	C-8, C-9, C-10, C-14, C-15	
14	2.86/36.2	H-13	C-9, C-15	3.37/37.4	H-13	C-9, C-13, C-15	H-17
17	7.13/115.4	H-20-NH	C-16, C-19	7.22/116.0		C-16, C-19	H-14
1-NH	13.05/-	H-4		-			
8-OH	13.25/-			-			
10-OH	10.76/-		C-9, C-10, C-11	-			
20-NH	12.70/-	H-17		-			

Table S5. ^{1}H and ^{13}C NMR spectroscopic data for **8** and **8′** (CD_3OD).

	8 and **8′**	
position	δ_C, type[a]	δ_H, mult (*J* in Hz)[b]
2 / 2′	120.1, C[c] / 120.2, C[d]	
3 / 3′	127.6, C[c] / 127.3, C[d]	
4 / 4′	104.8, CH / 104.8, CH	7.01, s / 6.98, s
5 / 5′	N.O.[f]	
6 / 6′	184.4, C / 184.5, C	
7 / 7′	110.2, C[g] / 110.2, C[h]	
8 / 8′	N.O.[f]	
9 / 9′	111.6, C[g] / 111.2, C[h]	
10 / 10′	163.0, C / 163.5, C	
11 / 11′	106.3, CH / 106.7, CH	6.57, d (9.0) / 6.43, d (9.0)
12 / 12′	132.5, CH / 132.3, CH	7.97, m[e] / 7.96, m[e]
13 / 13′	18.5, CH / 48.9, CH	6.37, dd (8.3, 3.2) / 6.32, dd, (8.3, 3.2)
14a / 14a′	43.3, CH / 43.4, CH	3.49, m[e] / 3.46, m[e]
14b / 14b′		3.16, dd (18.1, 3.2) / 3.10, dd (18.1. 3.2)
15 / 15′	190.6, C / 190.6, C	
16 / 16′	130.4, C / N.O.[f]	
17 / 17′	116.1, CH / 116.2, CH	6.76, s / 6.75, s
18 / 18′	116.6, C[i] / 116.8, C[j]	
19 / 19′	N.O.[i] / N.O.[j]	

[a]confirmed by HSQC and HMBC.[b]500MHz. [c,d,g,h,i,j]Signals may be switched. [e]Overlapping signals. [f]Not observed (N.O.).

Table S6. COSY, HMBC, and NOESY NMR data for **8** and **8′** (500 MHz, CD_3OD).

		8 and **8′**	
position	δ_H/δ_C	COSY / NOESY	HMBC
4	7.01/104.8	- / H-12	120.1, 127.6
4′	6.98/104.8	- / H-12	120.2, 127.3
11	6.57/106.3	H-12 / H-12	110.2, 111.6
11′	6.43/106.7	H-12′ / H-12′	111.2
12	7.97/132.5	H-11 / H-4, H-11	C-6, C-10
12′	7.96/132.3	H-11′ / H-4′, H-11′	C-6′, C-10′
13	6.37/48.5	H-14a, H-14b / H-14a, H-14b	
13′	6.32/48.9	H-14a′, H-14b′ / H-14a′, H-14b′	
14a	3.49/43.3	H-13, H-14b / H-13, H-14b	C-15
14a′	3.46/43.4	H-13′, H-14b′ / H-13′, H-14b′	C-15′
14b	3.16/43.3	H-13, H-13a / H-13, H-14a	
14b′	3.10/43.4	H-13′, H-13a′ / H-13′, H-14a′	
17	6.76/116.1		C-16, 116.6
17′	6.75/116.2		116.8

Table S7. ^{1}H NMR spectroscopic data for **9** and **10** (DMSO-d_6).

	9/10	**9/10**
position	δ_H, mult (*J* in Hz)[a]	δ_H, mult (*J* in Hz)[a]
4	7.57, s[a]	7.36, br. s[c]
7	6.91, s[a]	7.20, br. s[c]
13	8.16, d (7.6)[b]	7.99, br. s[c]
14	7.51, d (7.6)[b]	6.89, br. s[c]
17	6.84, s[a]	6.52, br. s[c]

[a]500 MHz. [a,b,c]Signals may be switched.

Table S8. ^{1}H and ^{13}C NMR spectroscopic data for **13** (DMSO-d_6).

	13	
position	δ_C, type[a]	δ_H, mult (*J* in Hz)[a]
2, 3, 5, 6, 18, 19[c]		
4	108.0, CH	6.85, s
7	101.5, CH	6.66, s
8	158.6, C[d]	
9	110.7, C[d]	
10	166.2, C[d]	
11	105.2, C	
12	160.3, C	
13	132.8, CH	7.98, d (15.8)
14	122.7, CH	7.75, d (15.8)
15	178.1, C	
16	131.0, C	
17	114.7, CH	7.09, s

[a]500 MHz. [c]δ_C = 109.6, 112.4, 116.2, 120.0, 131.0, 131.6, 136.5. [d] Signals may be switched.

Table S9. COSY and HMBC NMR spectroscopic data for **13** (500 MHz, DMSO-d_6).

	13		
position	δ_H/δ_C	COSY	HMBC
4	6.85/108.0		112.4, 131.6
7	6.66/101.5		131.6, C-8, C-9, C-10, C-11
13	7.98/132.8	H-14	C-8, C-10, C-14, C-15
14	7.75/122.7	H-13	C-9, C-15
17	7.09/114.7		120.0, C-16

Supplementary Figures

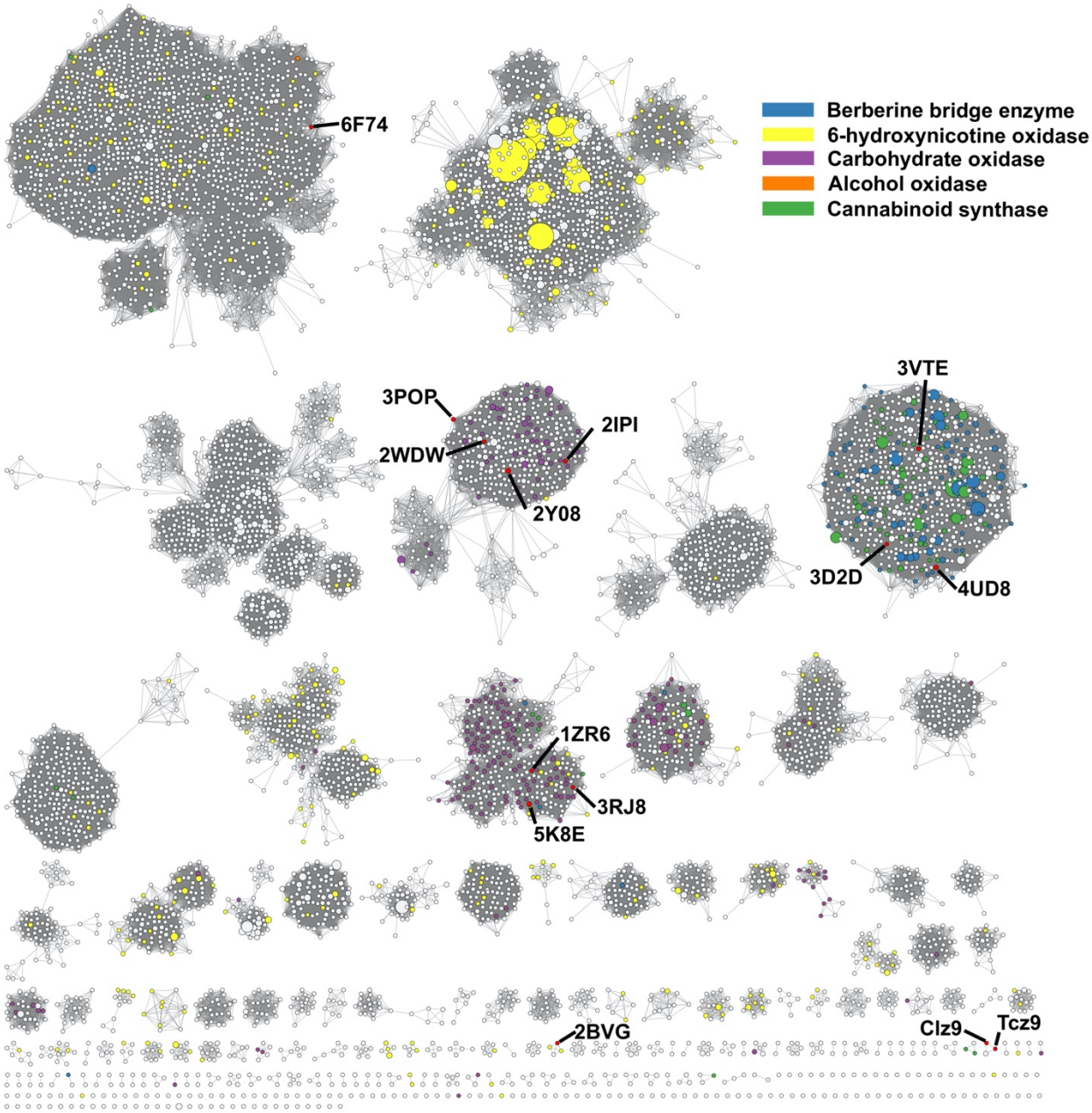

Figure S1. Sequence similarity network (SSN) of BBE-like oxidoreductases (Pfam PF08031 supplemented with Tcz9). SSN was generated by the EFI-EST[5] server at an E-value of 5 and alignment score of 85. The SSN was visualized using Cytoscape v3.8.0.[6] Proteins are colored by their putative function. Representative examples of BBE-like oxidoreductases include: 6F74, VAO-type oxidase (MtVAO713); 3POP, pregilvocarcin V oxidase (GilR); 2WDW, hexose oxidase (Dbv29); 2Y08, tirandamycin oxidase (TamL); 2IPI, aclacinomycin oxidoreductase (AknOx); 3VTE, tetrahydrocannabinolic acid synthase (THCA synthase); 3D2D, berberine bridge enzyme (EcBBE); 4UD8, monolignol oxidase (AtBBE); 1ZR6, glucooligosaccharide oxidase (GOOX); 5K8E, xylooligosaccharide oxidase (XylO); 3RJ8, carbohydrate oxidase; 2BVG, 6-hydroxy-D-nicotine oxidase (6-HDNO).

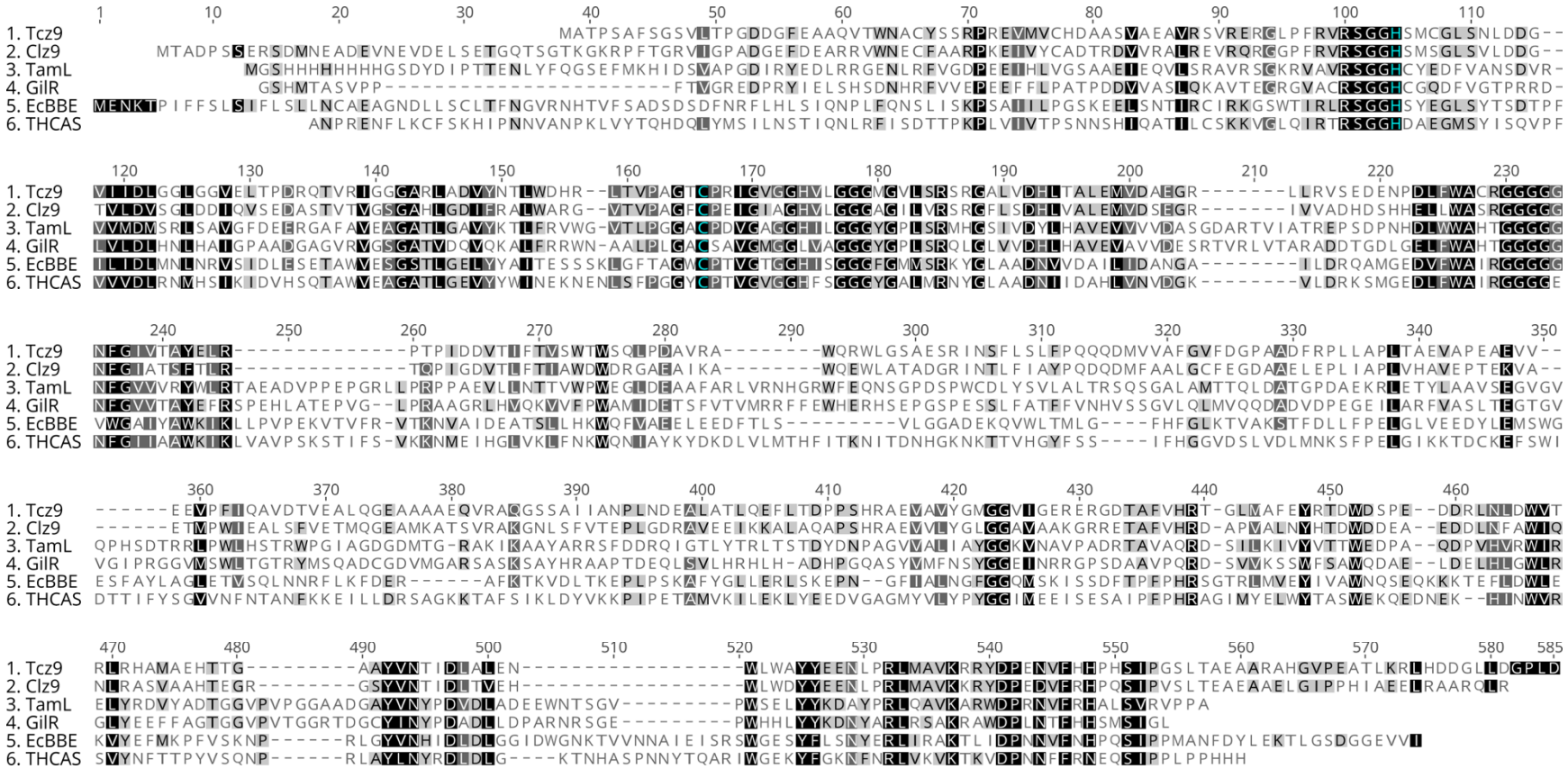

Figure S2. Sequence comparison of Tcz9 with related BBE-like oxidoreductases. The conserved histidine and cysteine residues responsible for bicovalent attachment with FAD are colored blue. Tcz9 from Actinomycete sp. AJS-327; Clz9 from *Streptomyces* sp. CNH-287; TamL, 10-hydroxy-dehydrogenase in tirandamycin biosynthesis from *Streptomyces* sp. 307-9 (2Y08); GilR, pregilvocarcin V oxidase in gilvocarcin biosynthesis from *Streptomyces griseoflavus* Gö 3592 (3POP); EcBBE, berberine bridge enzyme from *Eschscholzia californica* (3D2D); THCA_synthase, tetrahydrocannabinolic acid synthase from *Cannabis sativa* (3VTE). The alignment was performed using ClustalW[7] and Geneious Pro 2019.1.3 (https://www.geneious.com) for visualization of the results.

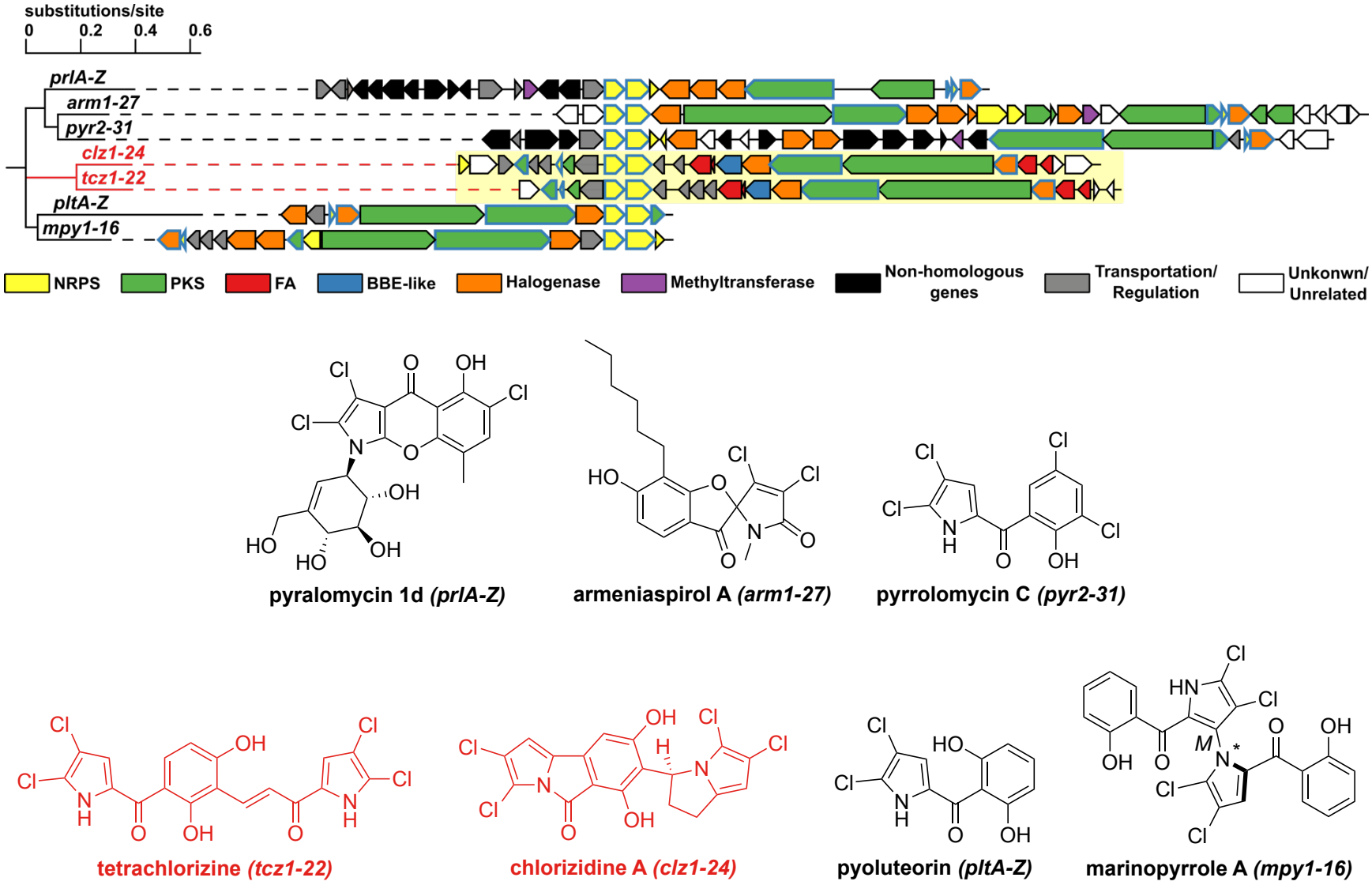

Figure S3. Alignment of characterized BGCs associated with dichloropyrrole-containing natural products using CORASON.[8] BGCs compared in this study (*tcz* and *clz*) are highlighted in yellow. Biosynthetic genes conserved across each BGC (core genes) are outlined in blue. BGCs are aligned by the conserved adenyl-transferase (AT) gene and referenced to the *clz* gene cluster. Branch length is calculated by concatenation and alignment of the conserved biosynthetic genes. E-value is 40.

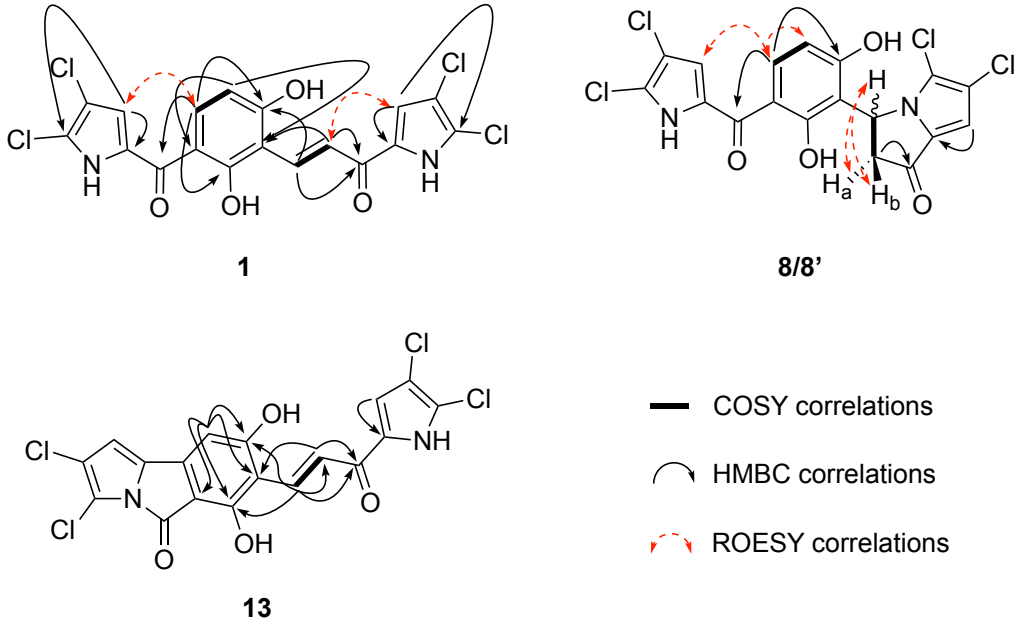

Figure S4. Key absolute COSY, ROESY, and HMBC correlations for **1, 8**, and **13**. Correlations between protons and ambiguous carbons are listed in Tables S6 and S9.

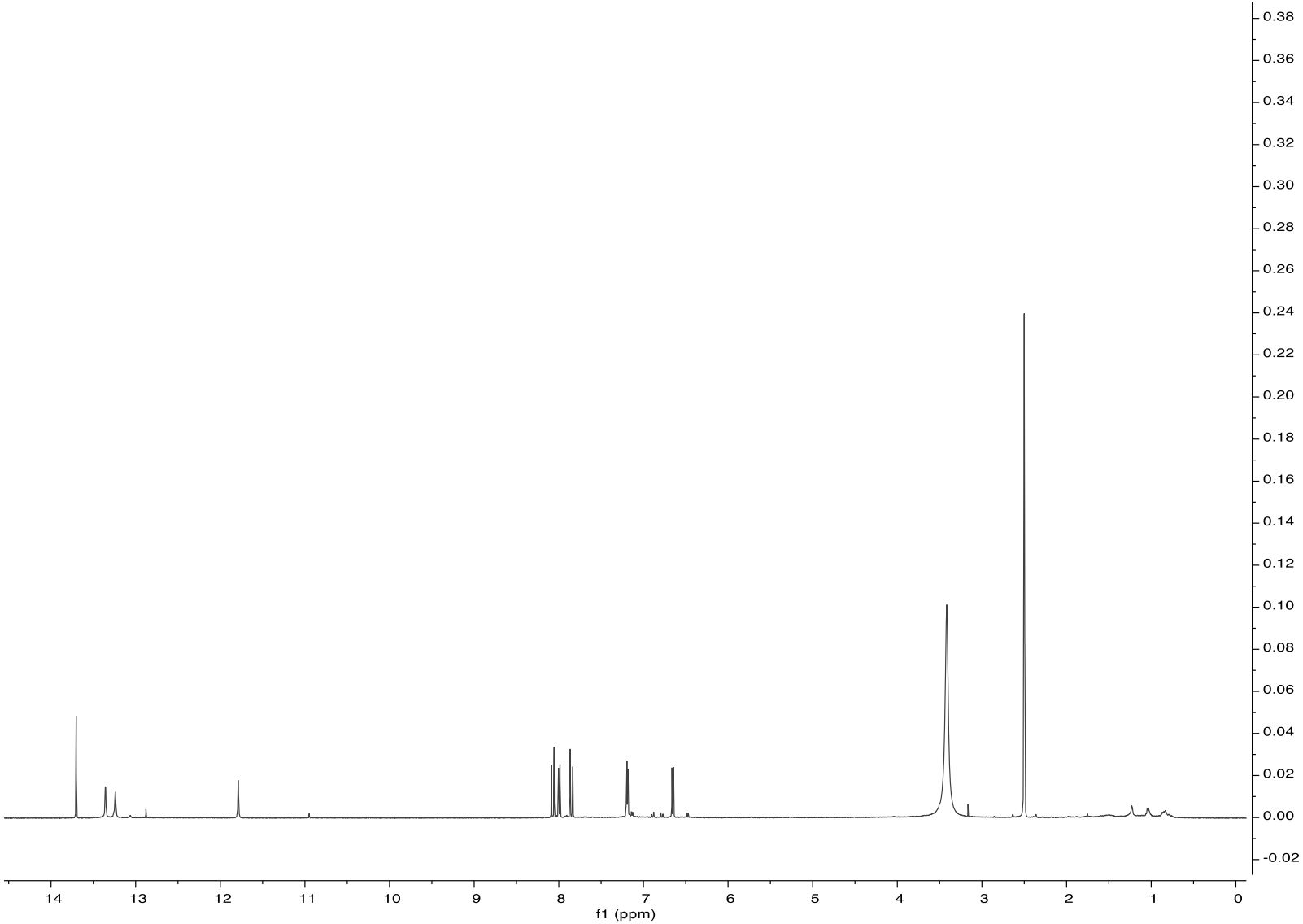

Figure S5. ^{1}H NMR spectrum of tetrachlorizine (**1**) in DMSO-d_6.

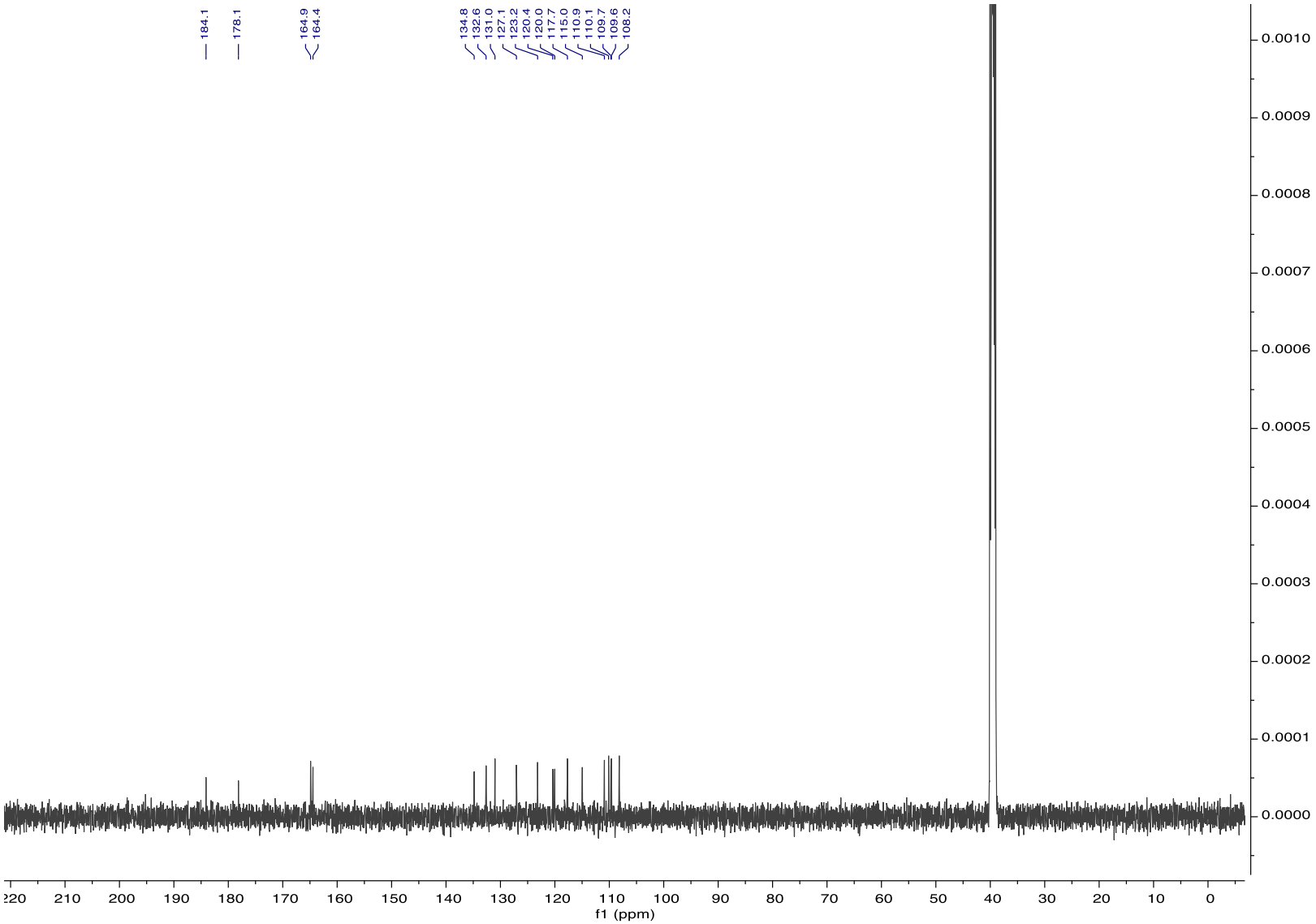

Figure S6. ^{13}C NMR spectrum of tetrachlorizine (**1**) in DMSO-d_6.

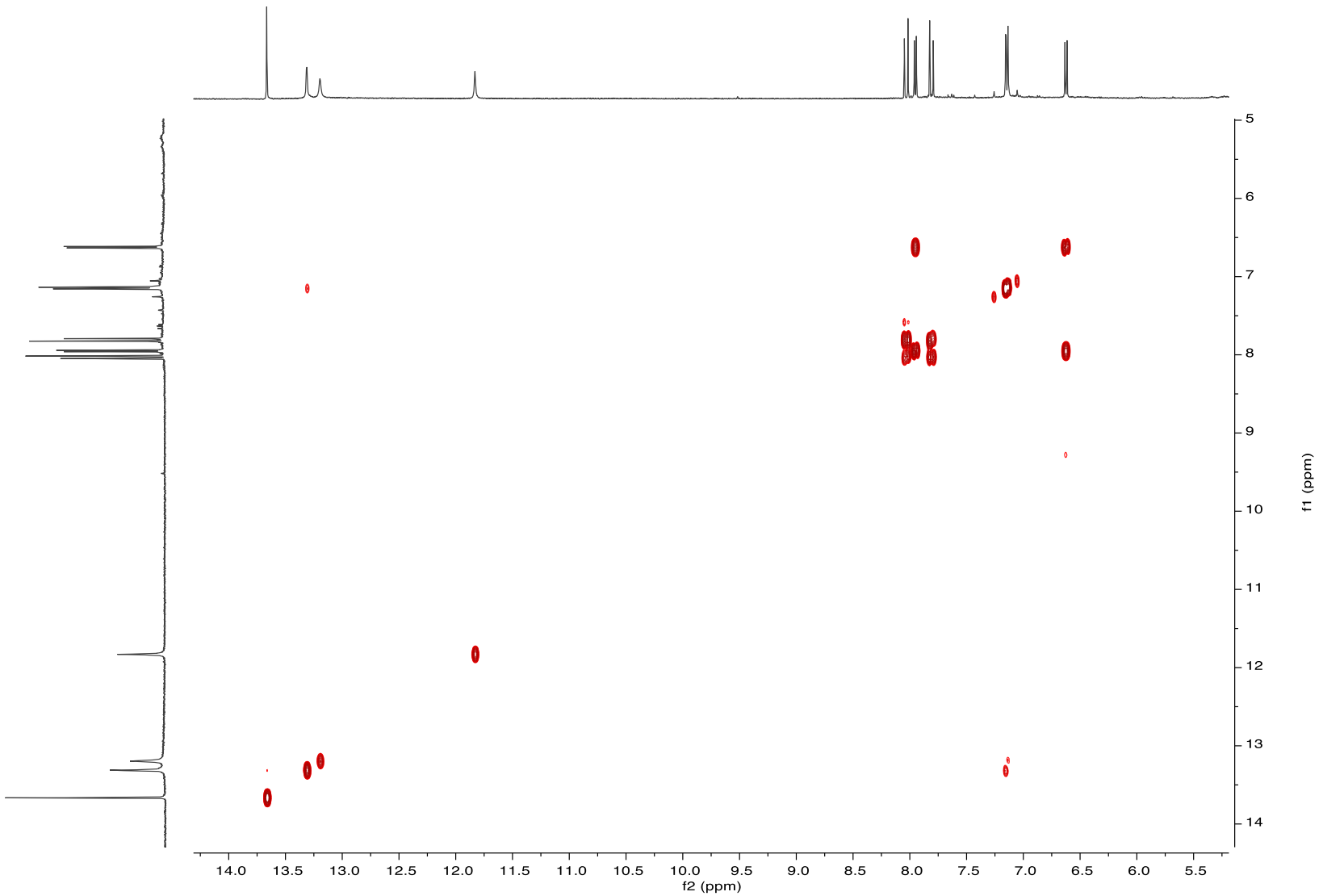

Figure S7. COSY NMR spectrum of tetrachlorizine (**1**) in DMSO-d_6.

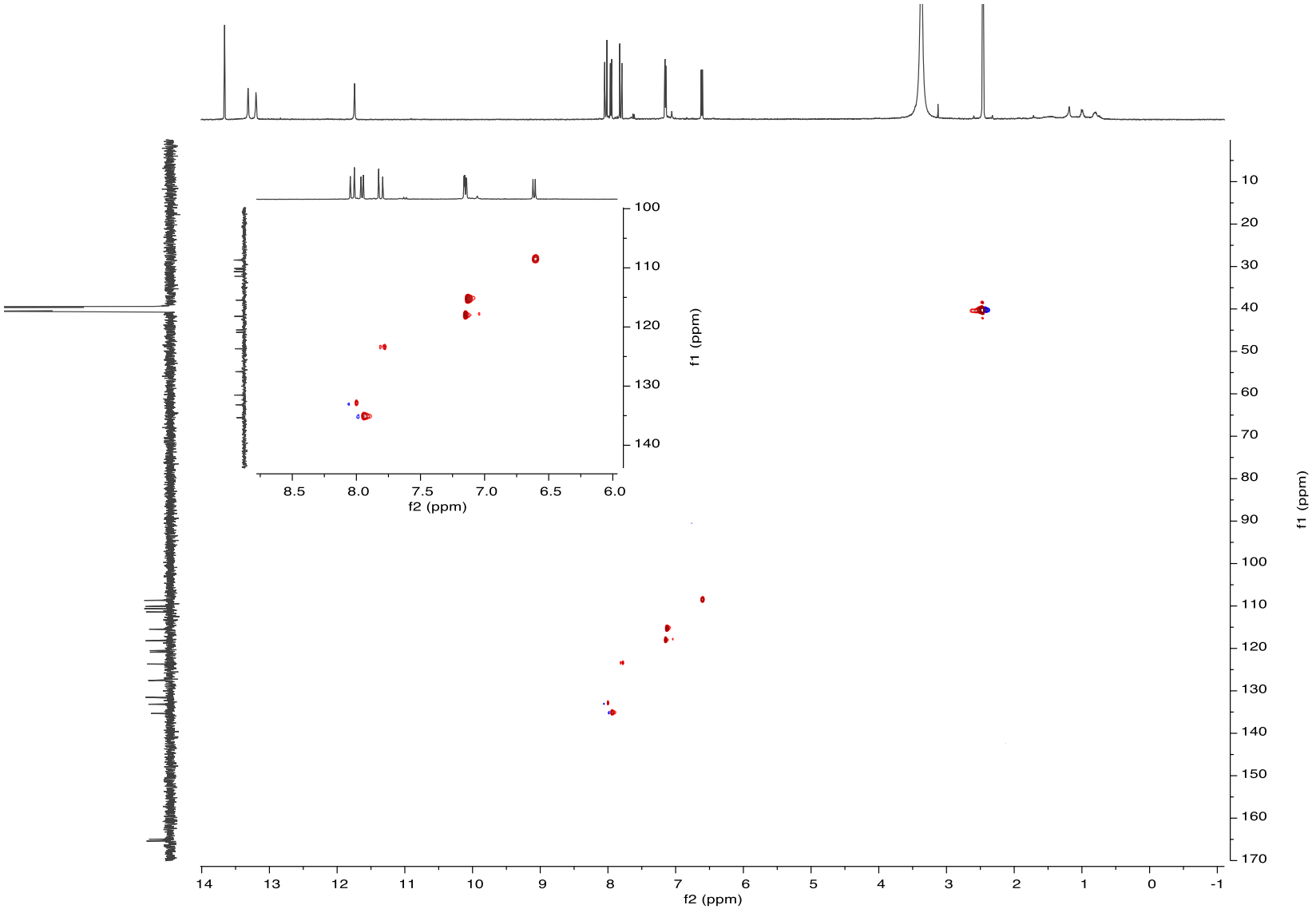

Figure S8. HSQC NMR spectrum of tetrachlorizine (**1**) in DMSO-d_6.

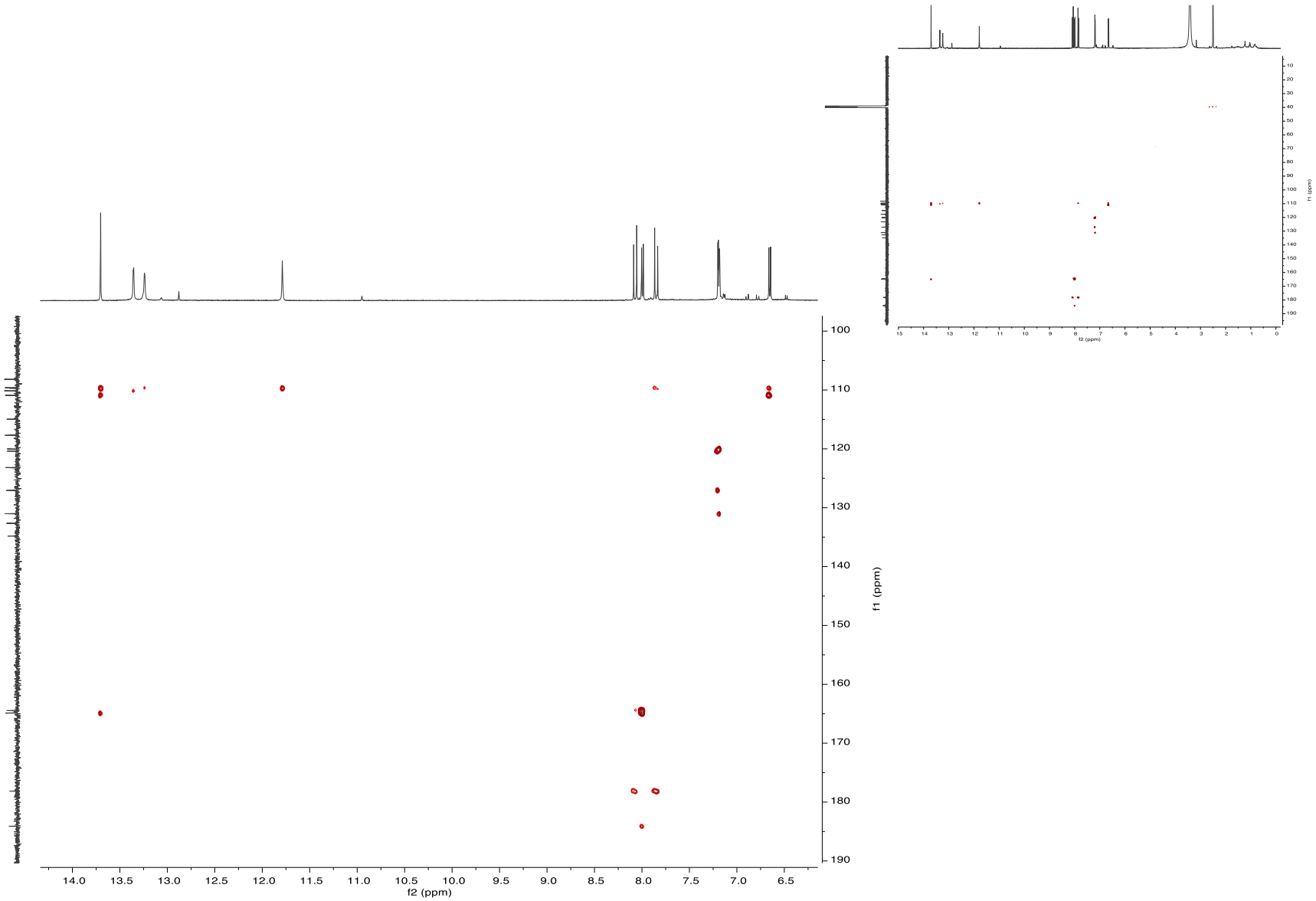

Figure S9. HMBC NMR spectrum of tetrachlorizine (**1**) in DMSO-d_6.

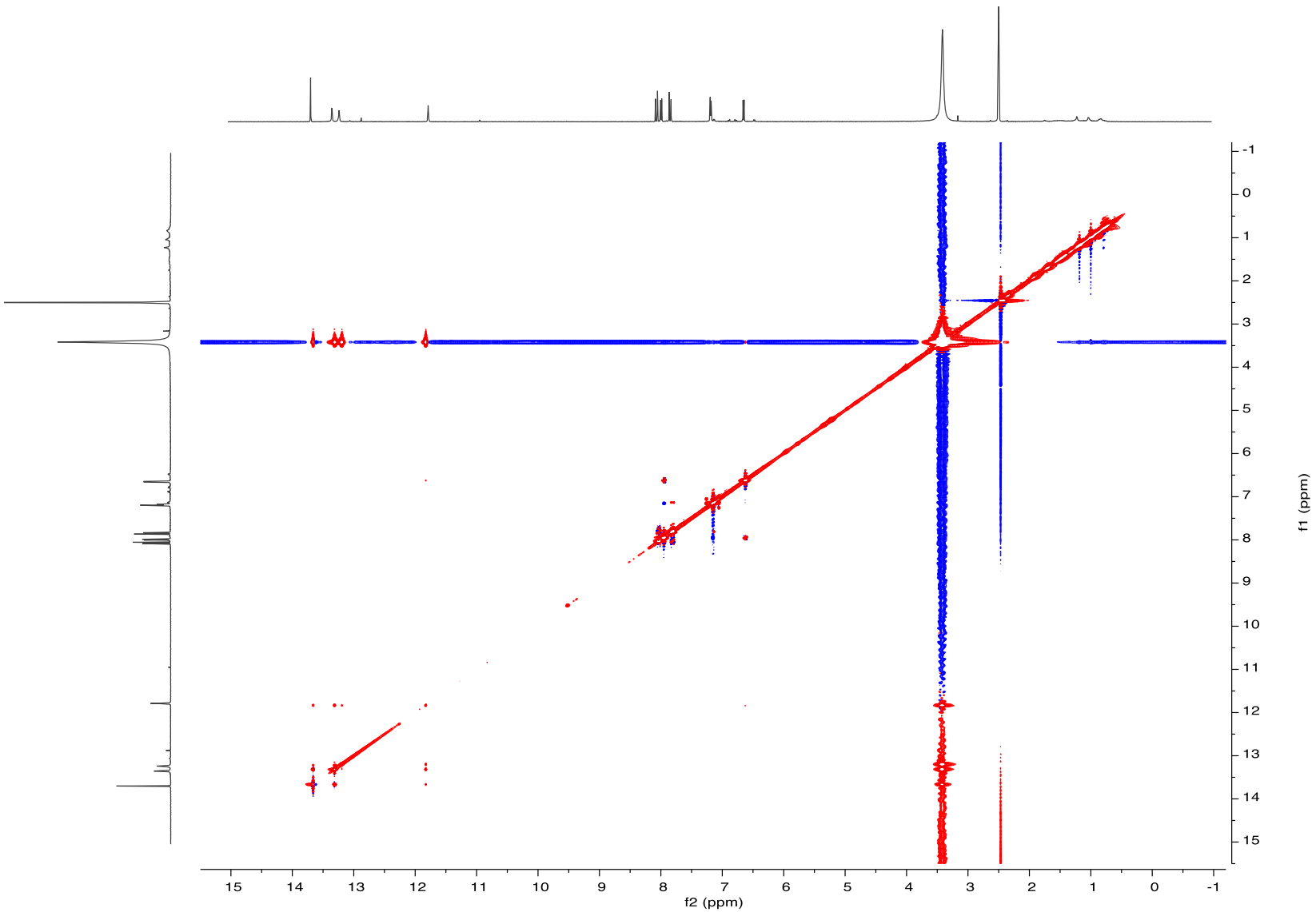

Figure S10. ROESY NMR spectrum of tetrachlorizine (**1**) in DMSO-d_6.

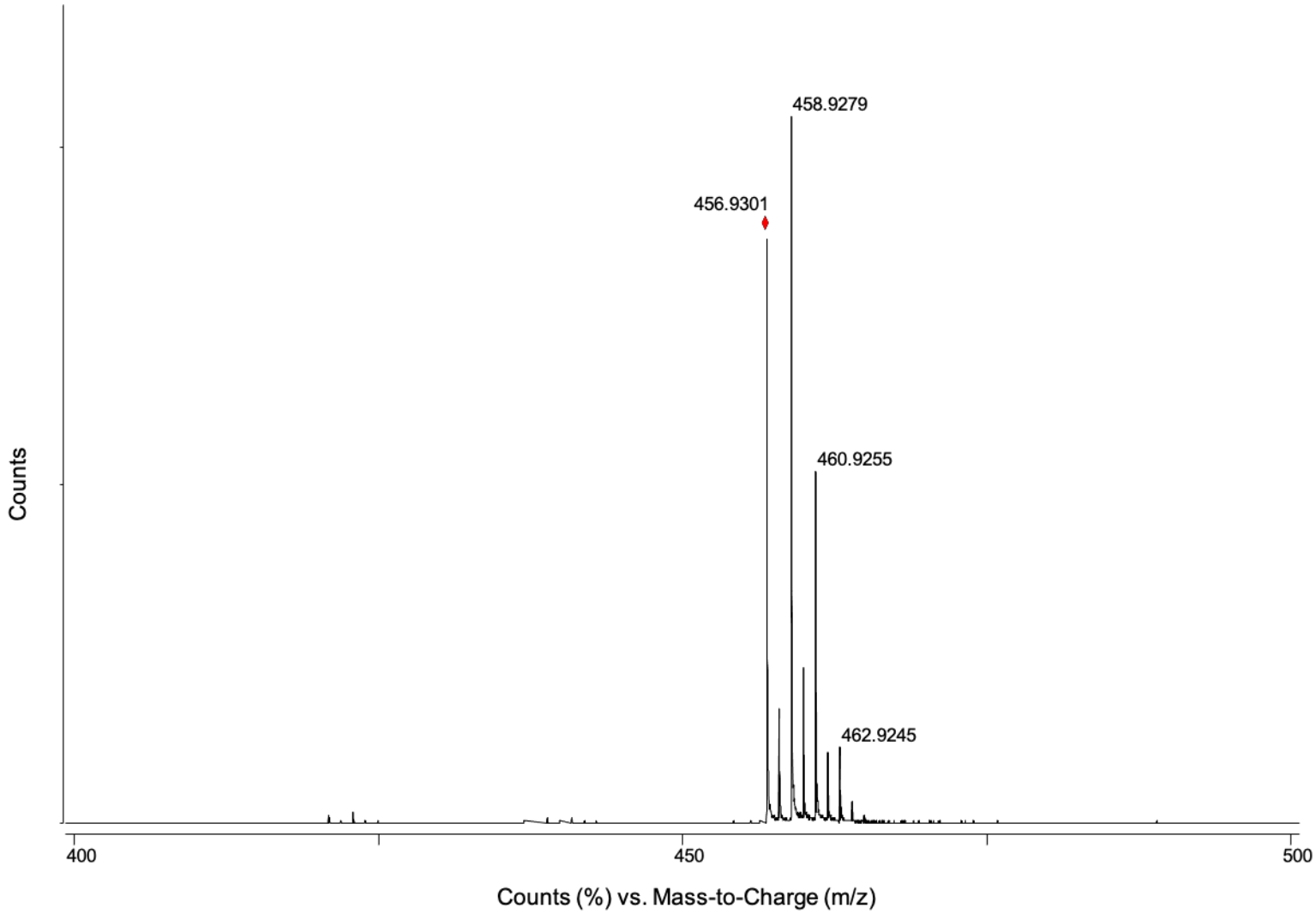

Figure S11. HR-ESI-TOF-MS spectrum of tetrachlorizine (**1**).

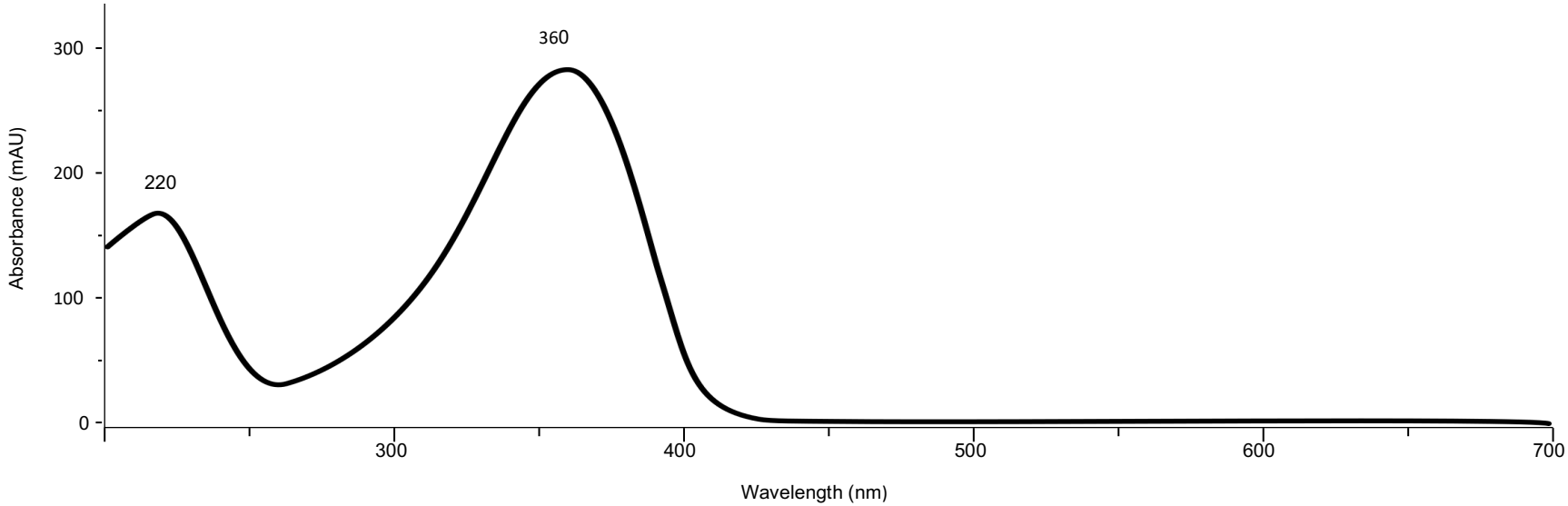

Figure S12. UV/vis spectrum of tetrachlorizine (**1**) (CH_3OH).

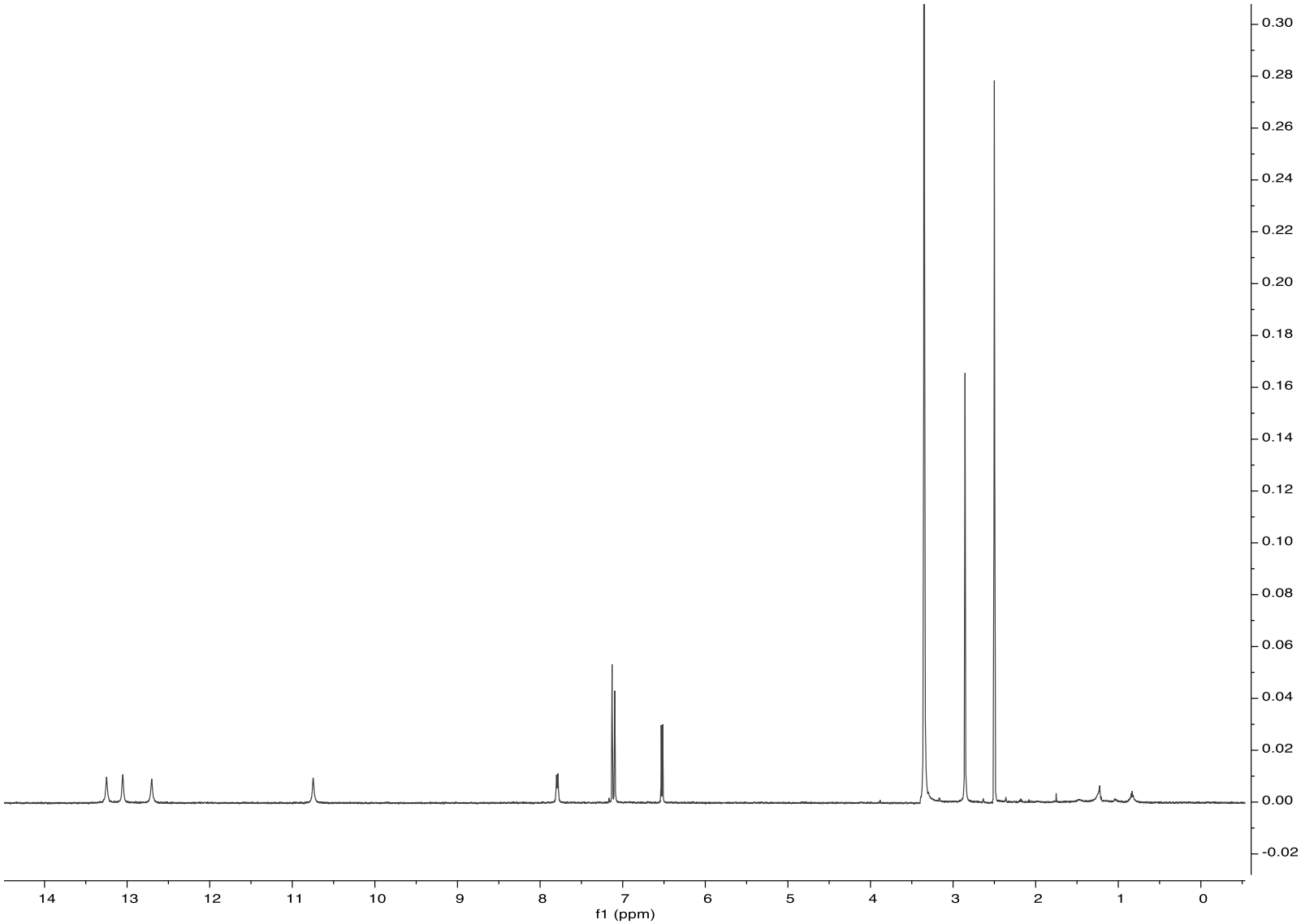

Figure S13. ^{1}H NMR spectrum of dihydrotetrachlorizine (**2**) in DMSO-d_6.

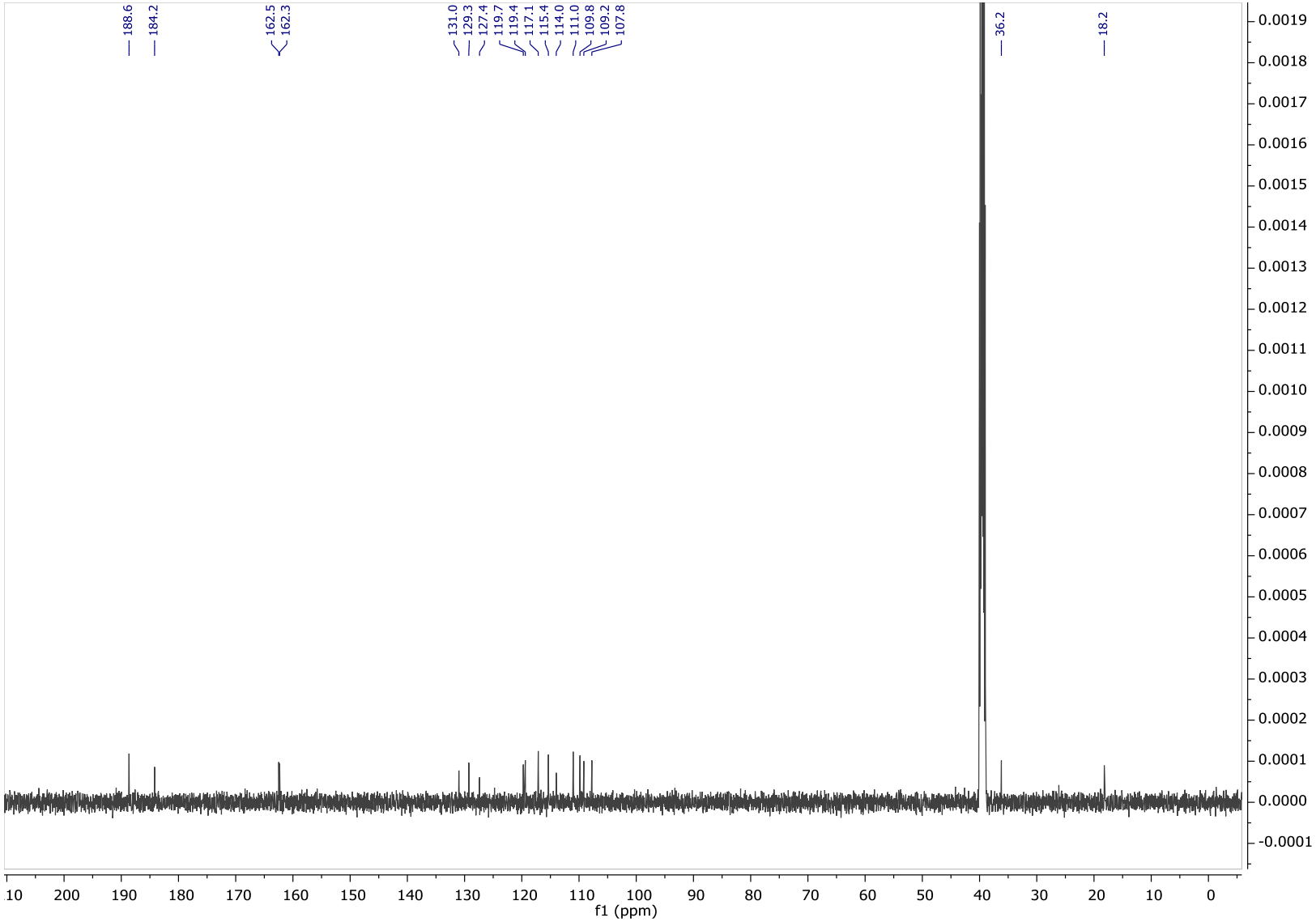

Figure S14. ^{13}C NMR spectrum of dihydrotetrachlorizine (**2**) in DMSO-d_6.

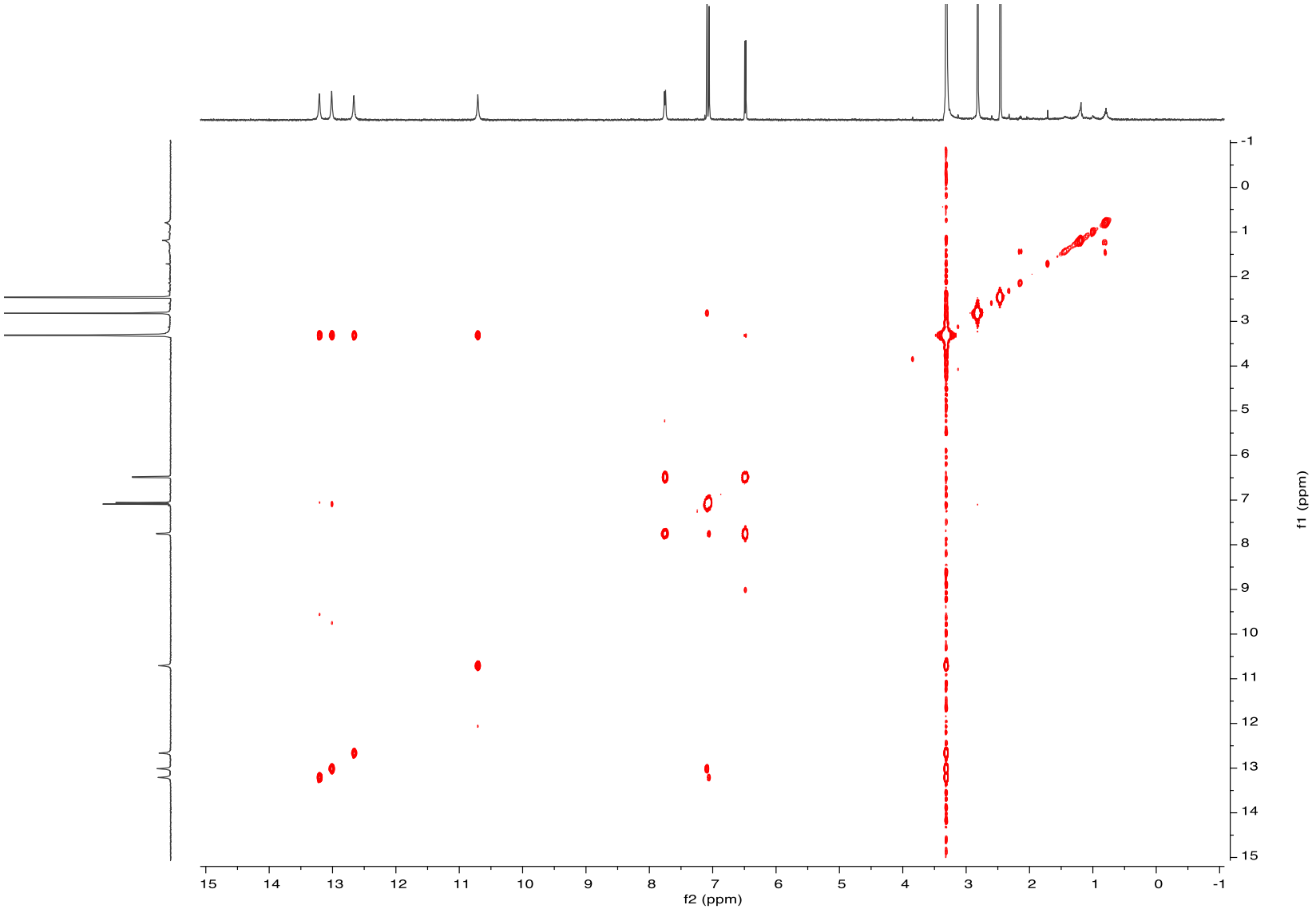

Figure S15. COSY NMR spectrum of dihydrotetrachlorizine (**2**) in DMSO-d_6.

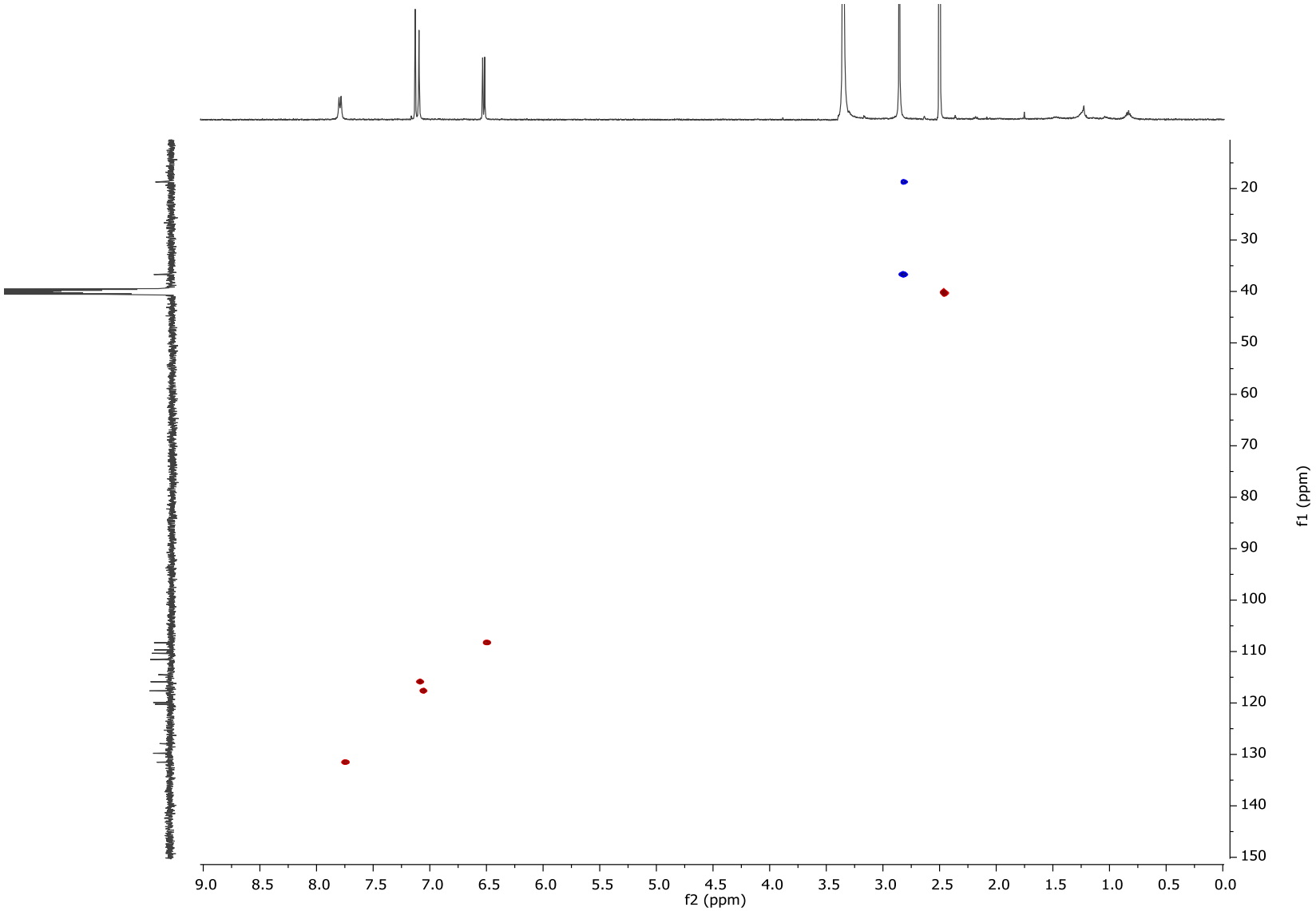

Figure S16. HSQC NMR spectrum of dihydrotetrachlorizine (**2**) in DMSO-d_6.

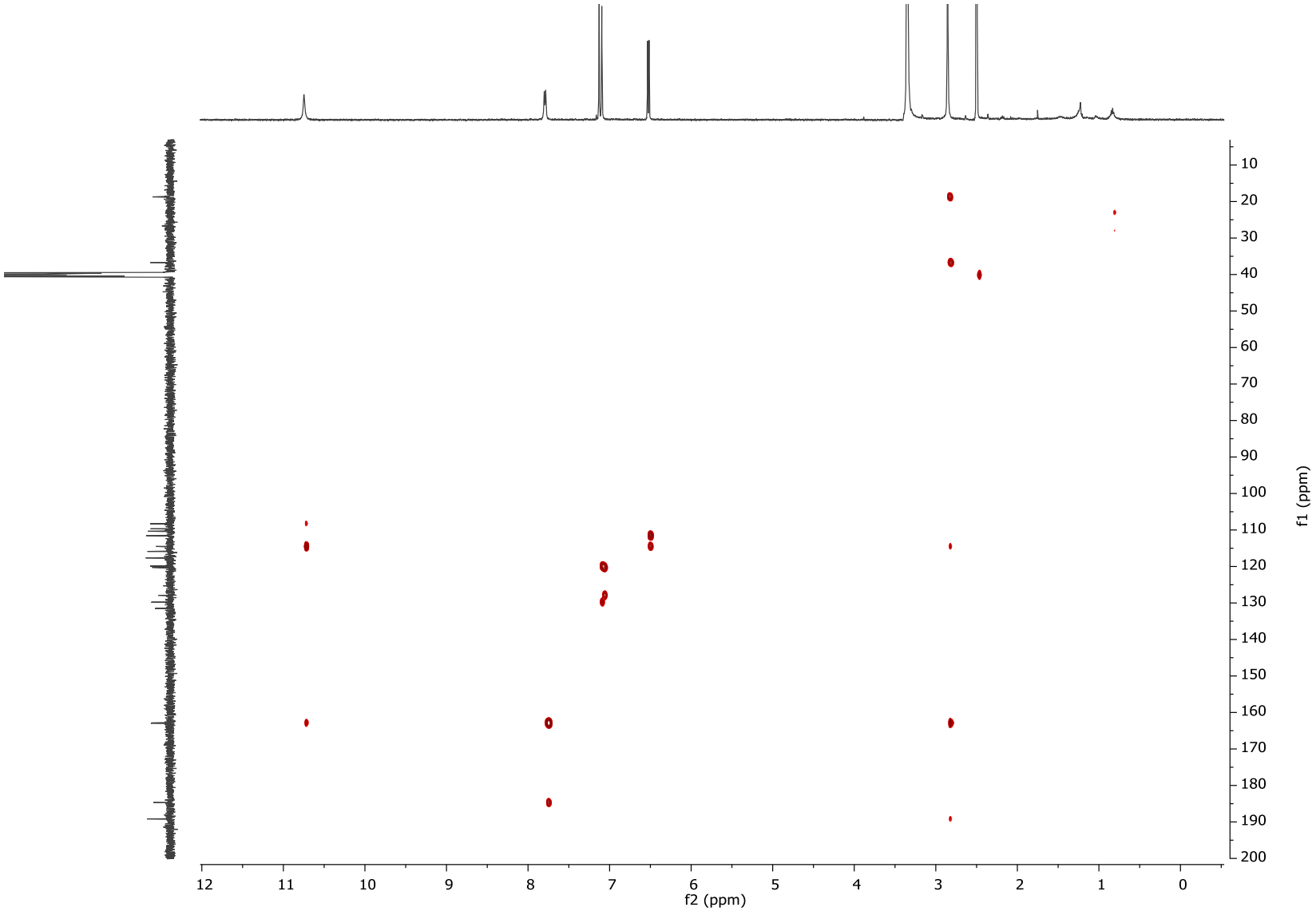

Figure S17. HMBC NMR spectrum of dihydrotetrachlorizine (**2**) in DMSO-d_6.

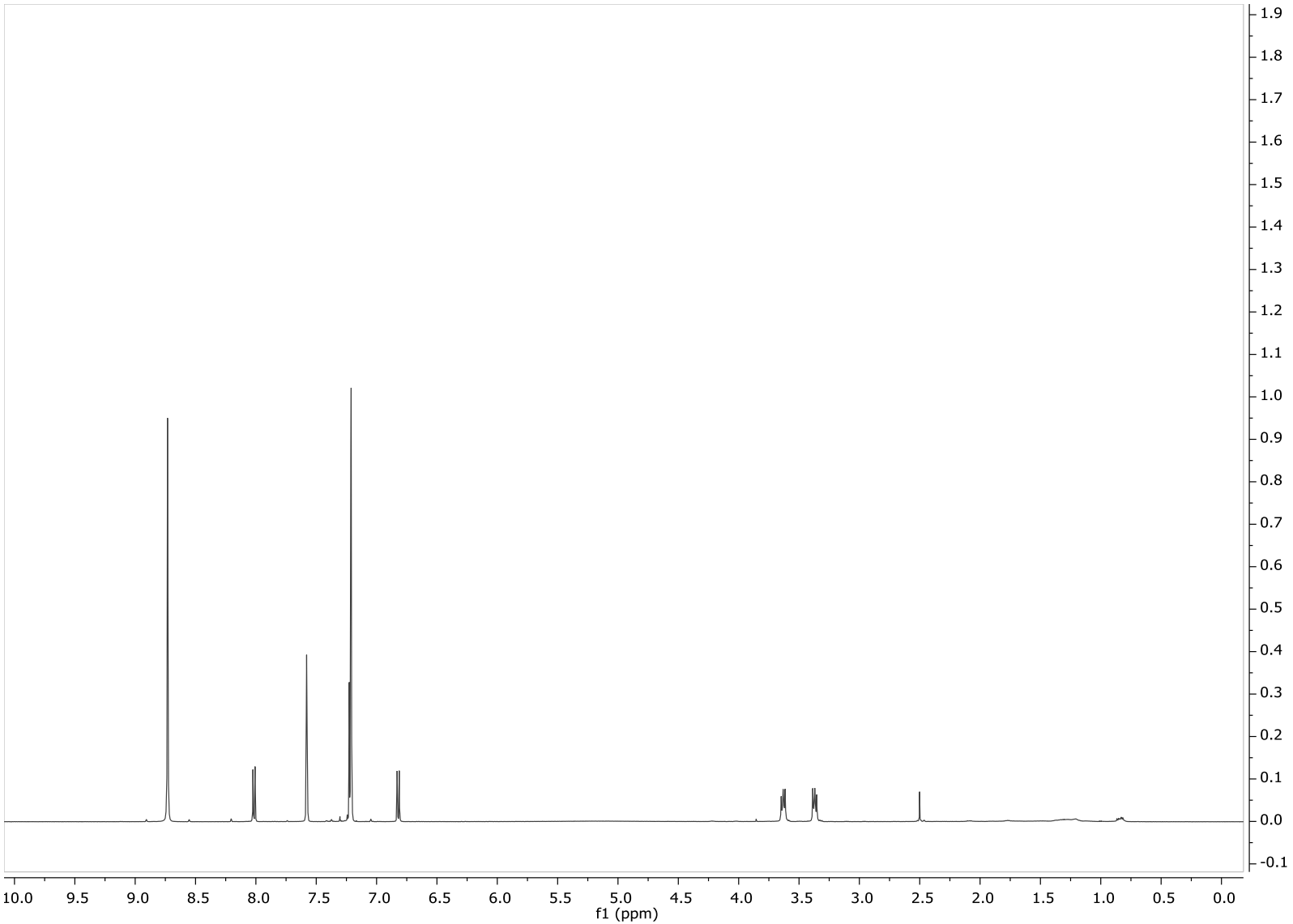

Figure S18. ^{1}H NMR spectrum of dihydrotetrachlorizine (**2**) in pyridine-d_5.

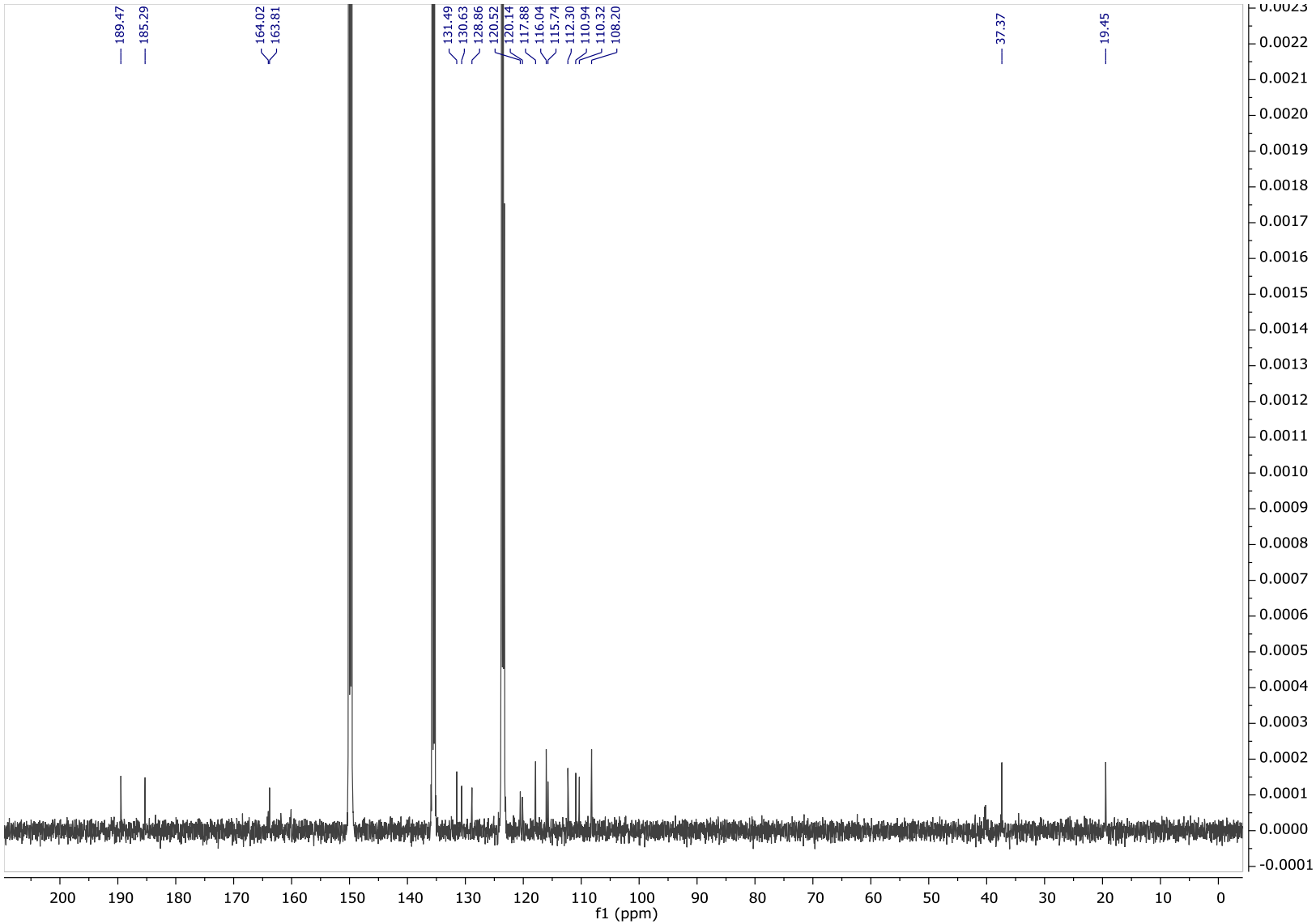

Figure S19. ^{13}C NMR spectrum of dihydrotetrachlorizine (**2**) in pyridine-d_5.

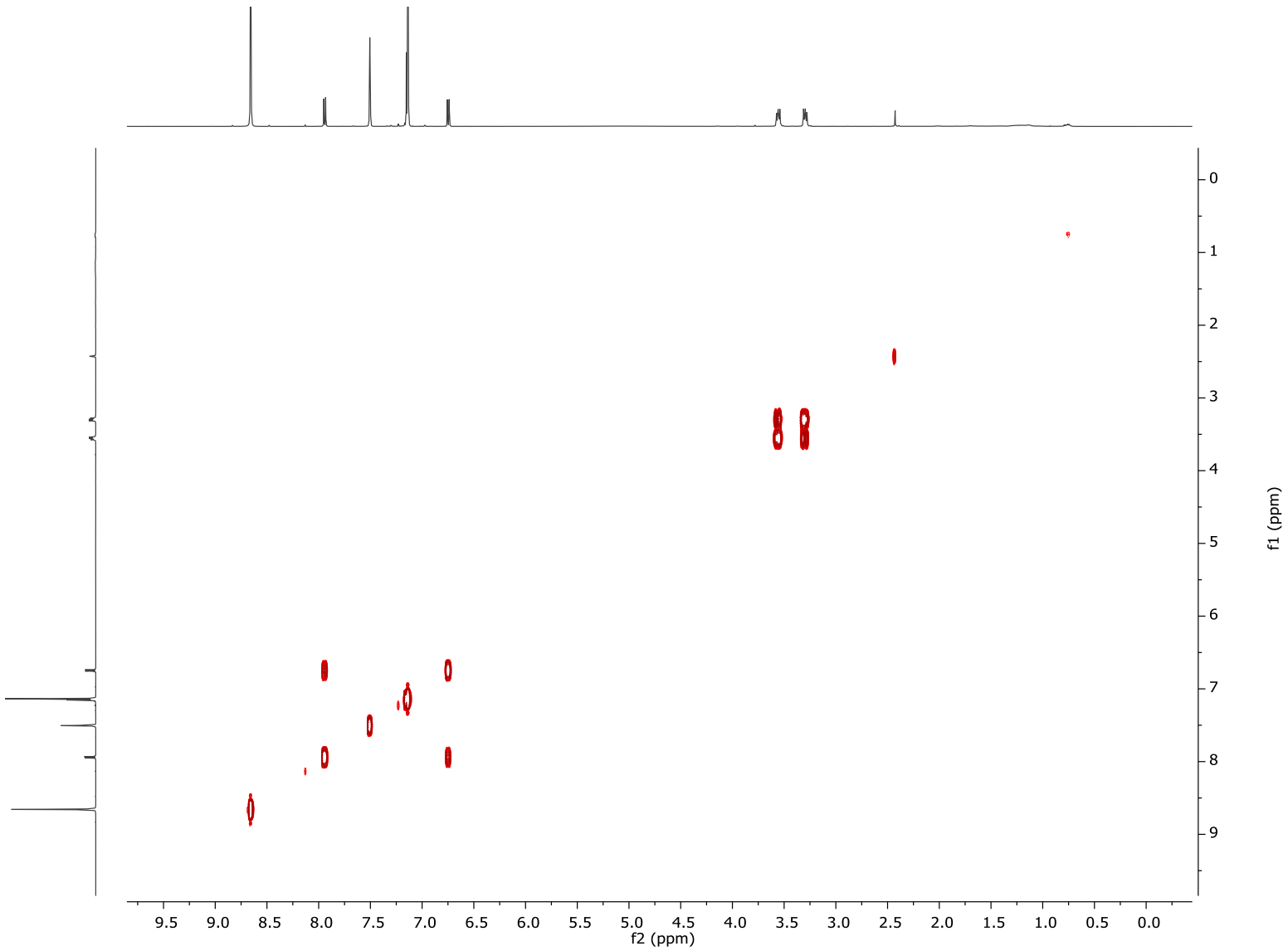

Figure S20. COSY NMR spectrum of dihydrotetrachlorizine (**2**) in pyridine-d_5.

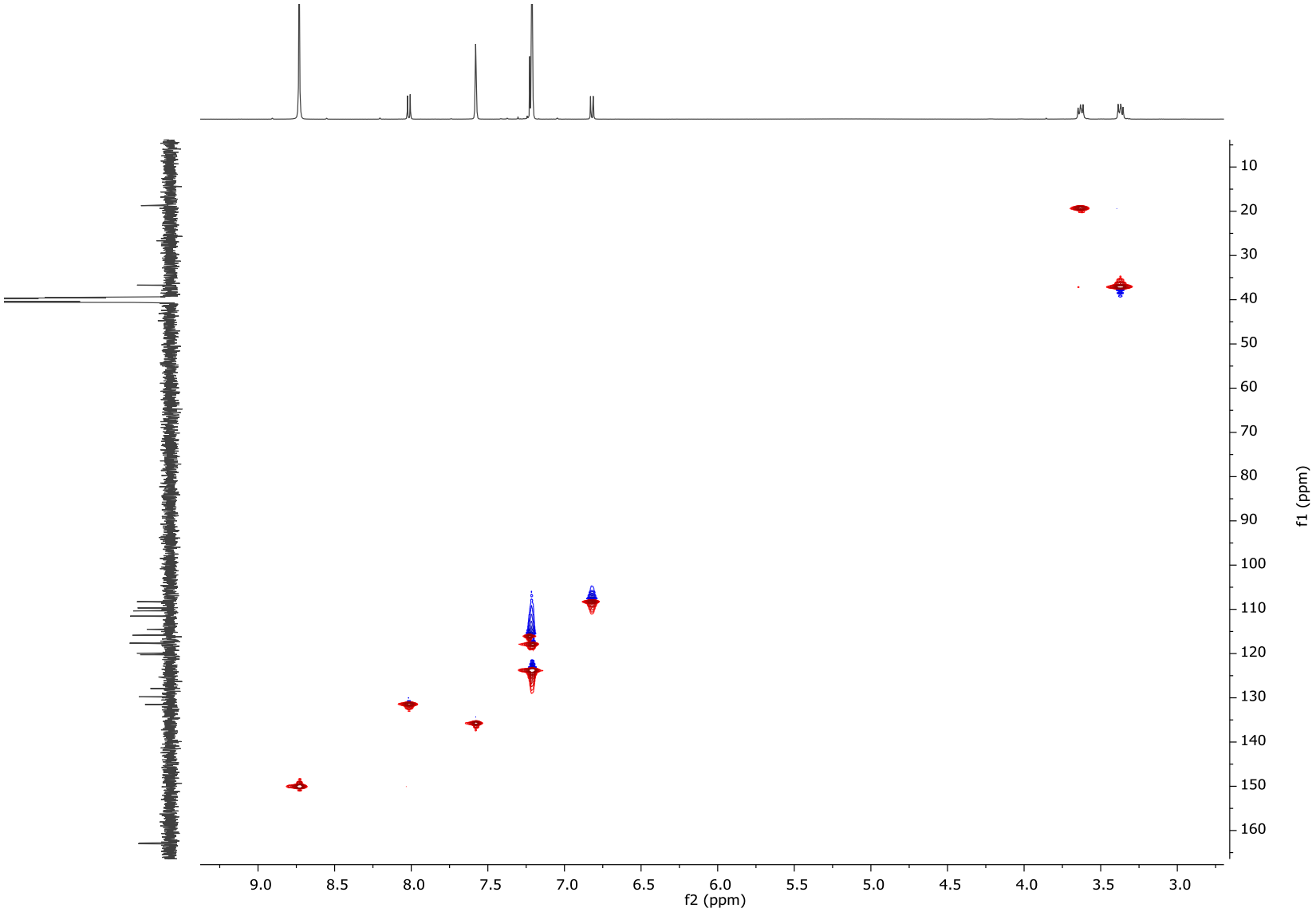

Figure S21. HSQC NMR spectrum of dihydrotetrachlorizine (**2**) in pyridine-d_5.

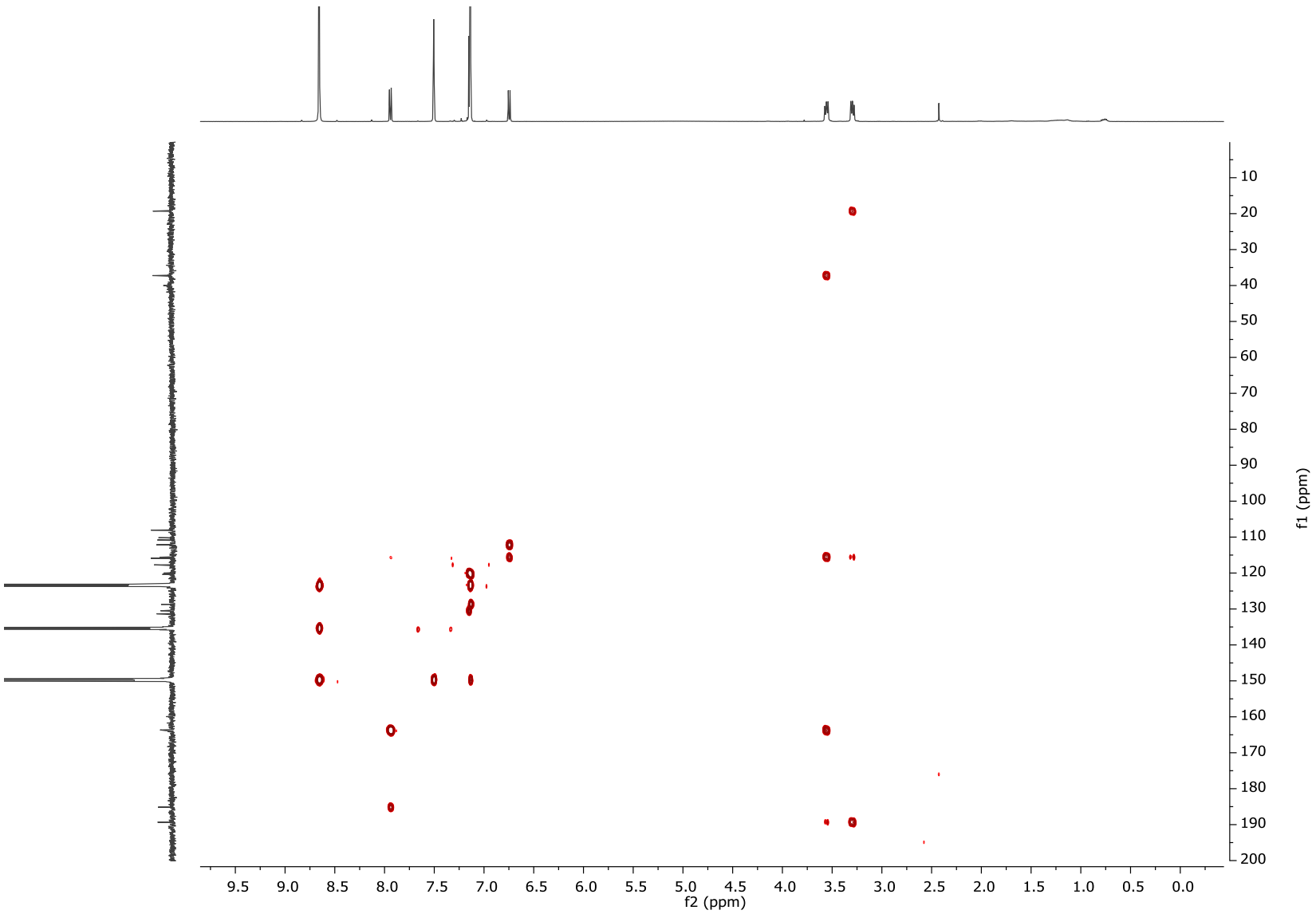

Figure S22. HMBC NMR spectrum of dihydrotetrachlorizine (**2**) in pyridine-d_5.

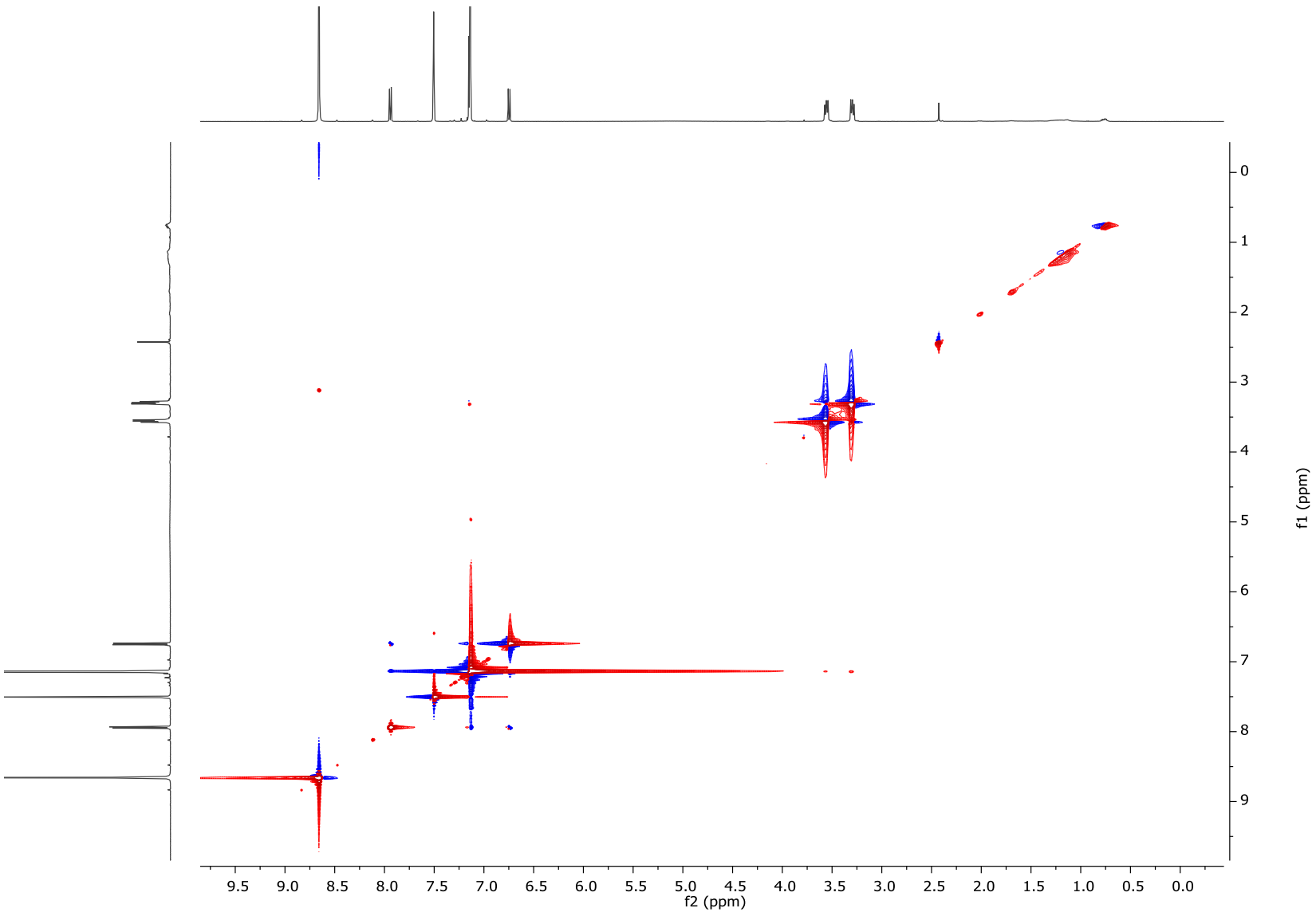

Figure S23. ROESY NMR spectrum of dihydrotetrachlorizine (**2**) in pyridine-d_5.

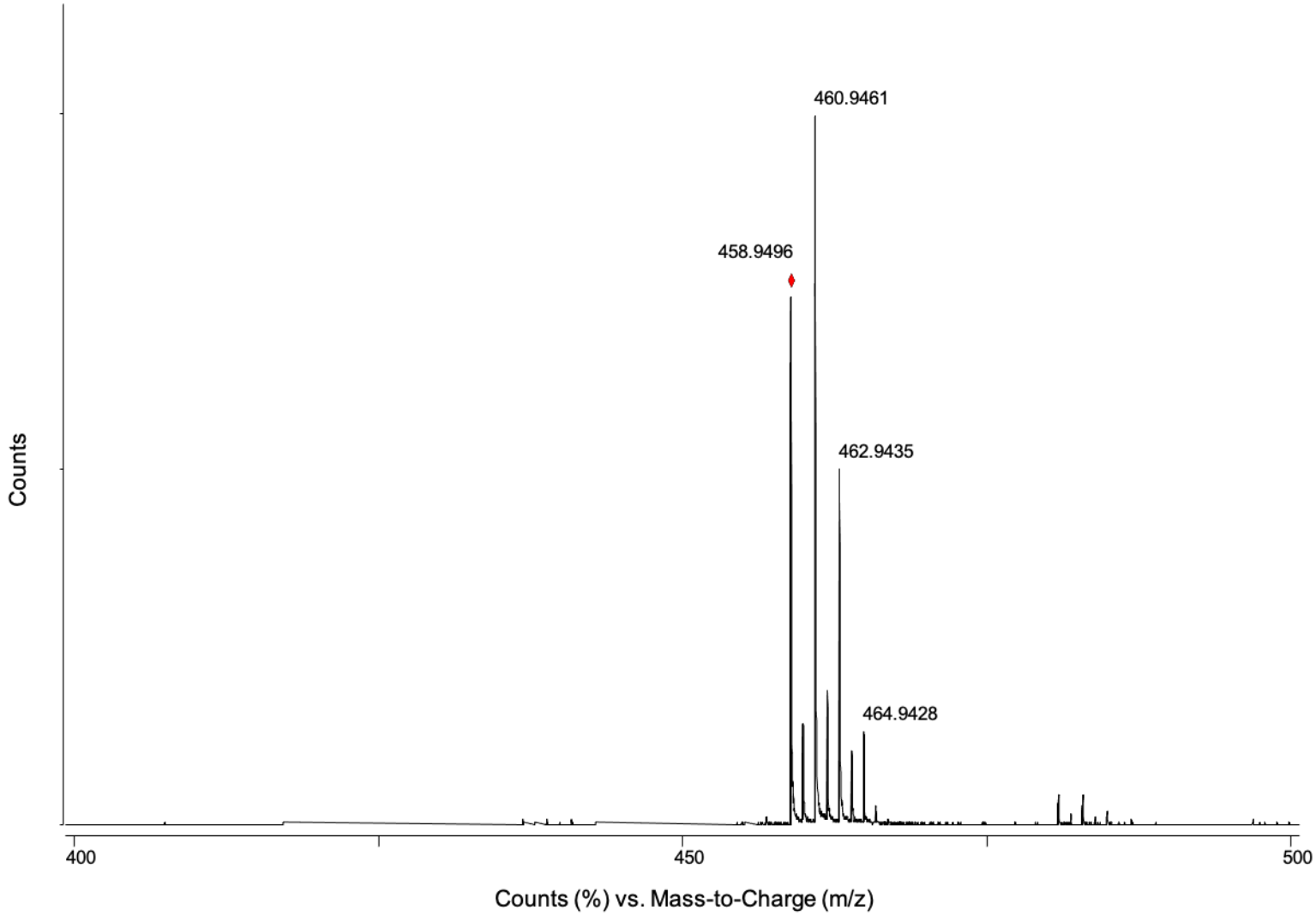

Figure S24. HR-ESI-TOF-MS spectrum of dihydrotetrachlorizine (**2**).

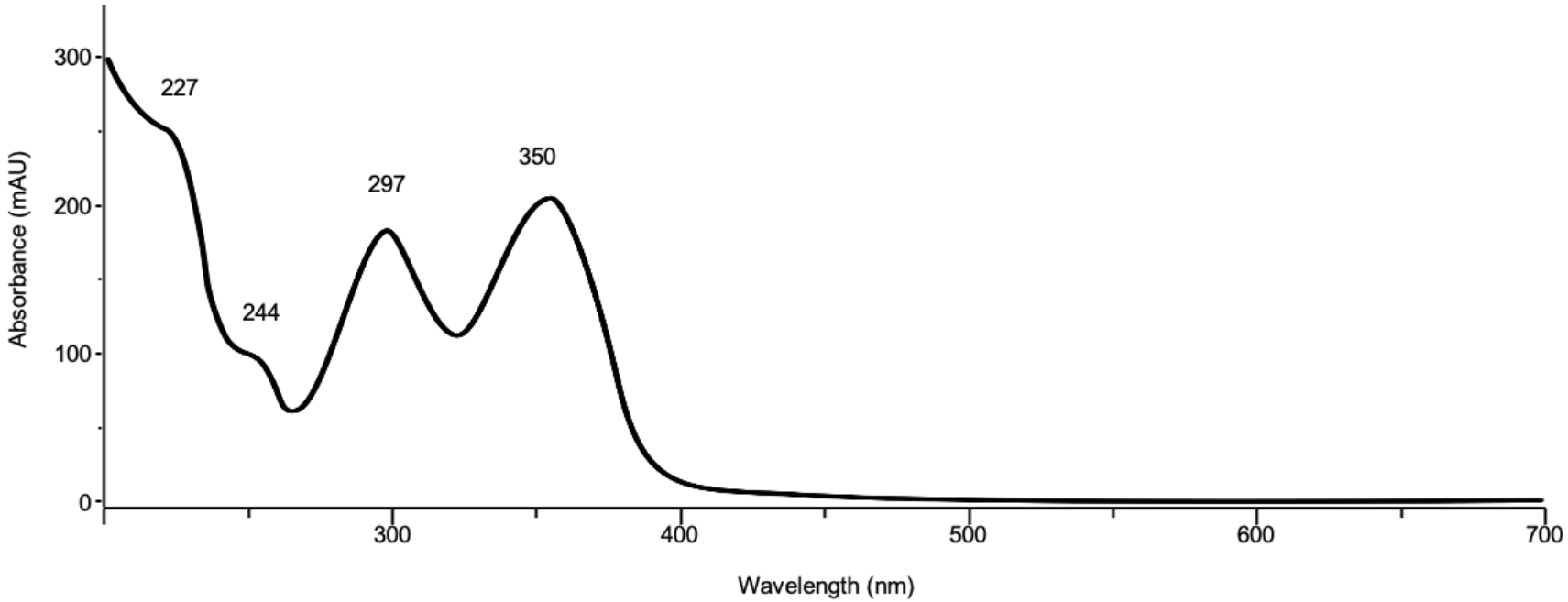

Figure S25. UV/vis spectrum of dihydrotetrachlorizine (**2**) (CH_3OH).

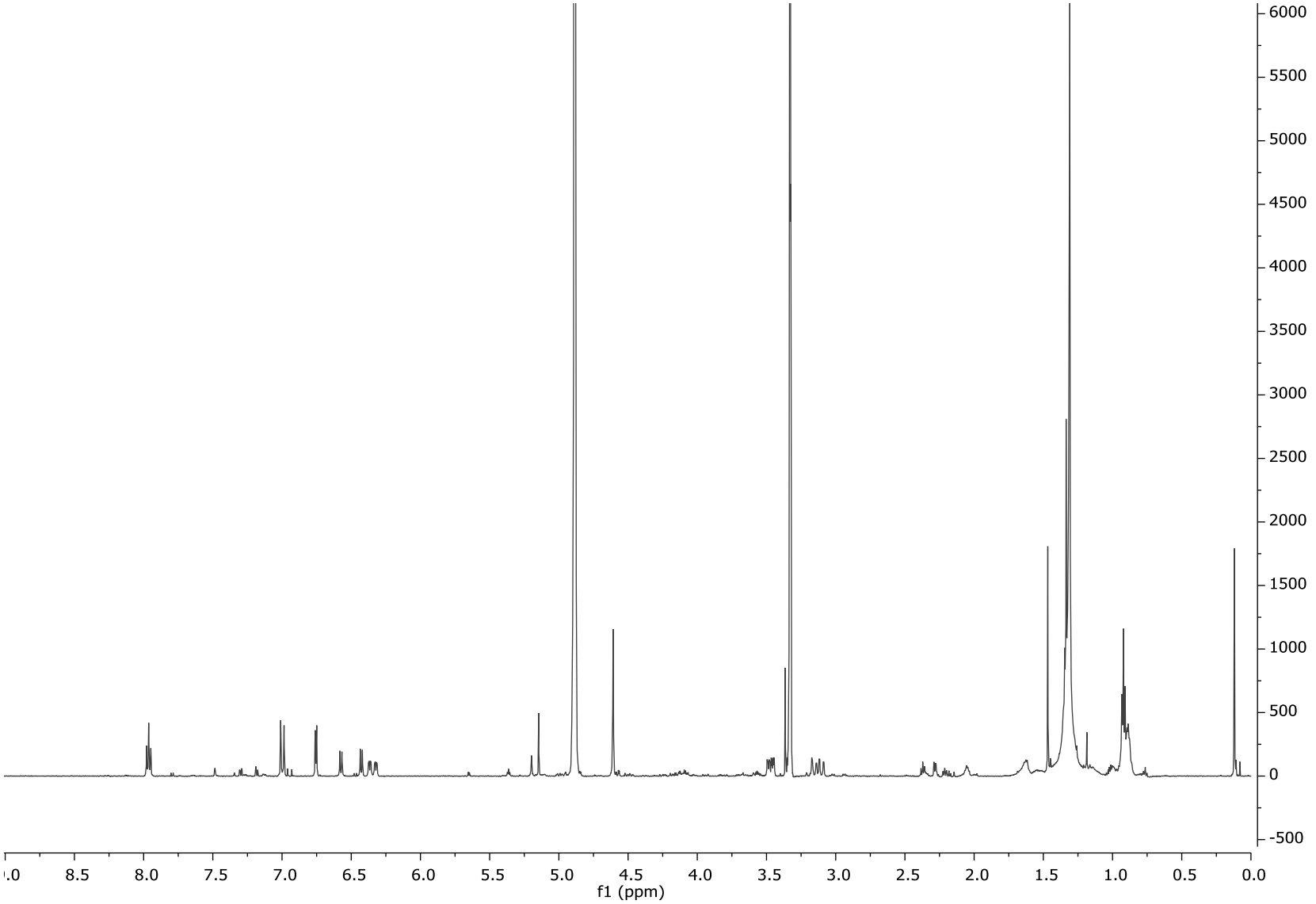

Figure S26. ^{1}H NMR spectrum of **8** in CD_3OD.

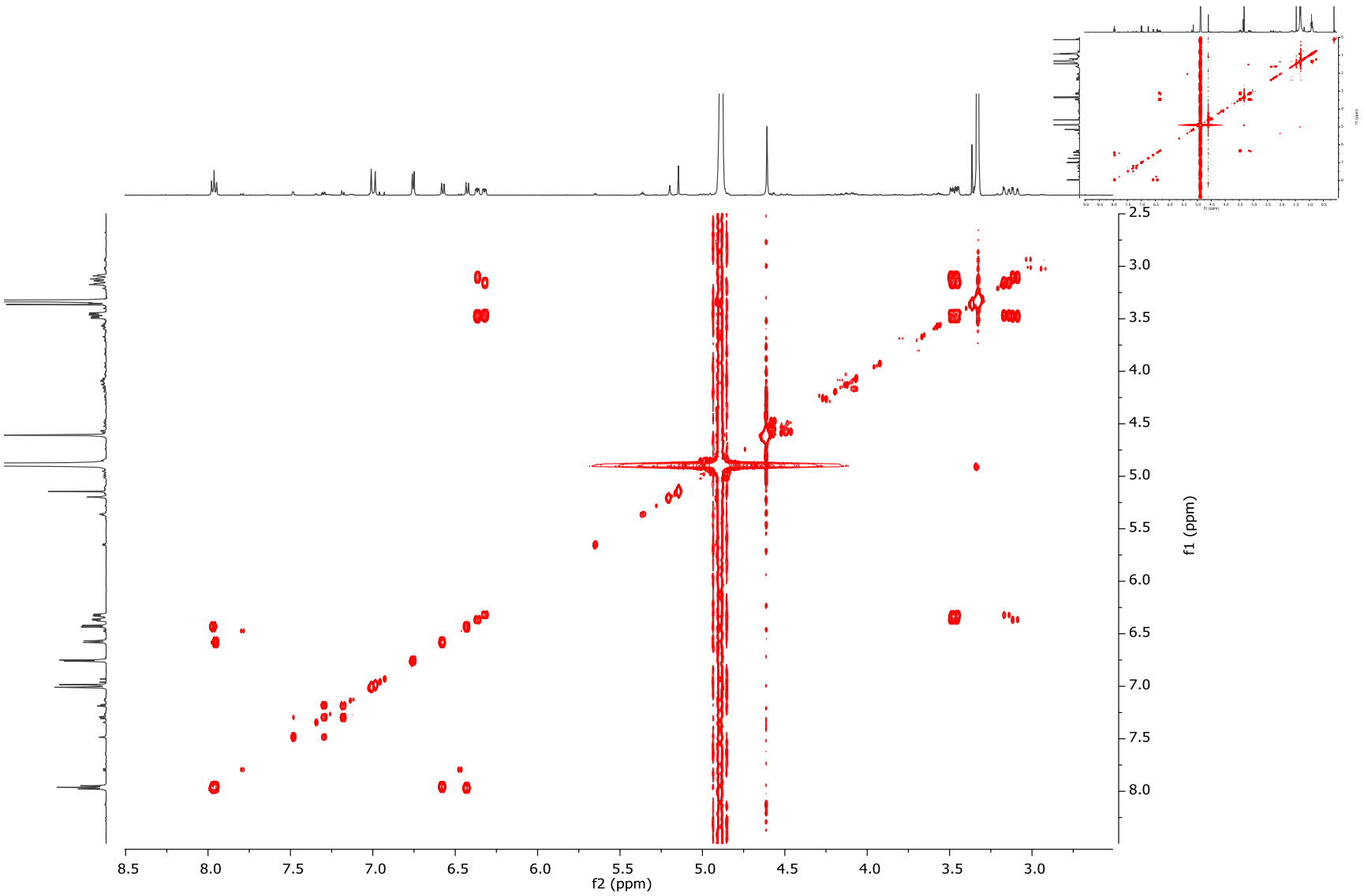

Figure S27. COSY NMR spectrum of **8** in CD_3OD.

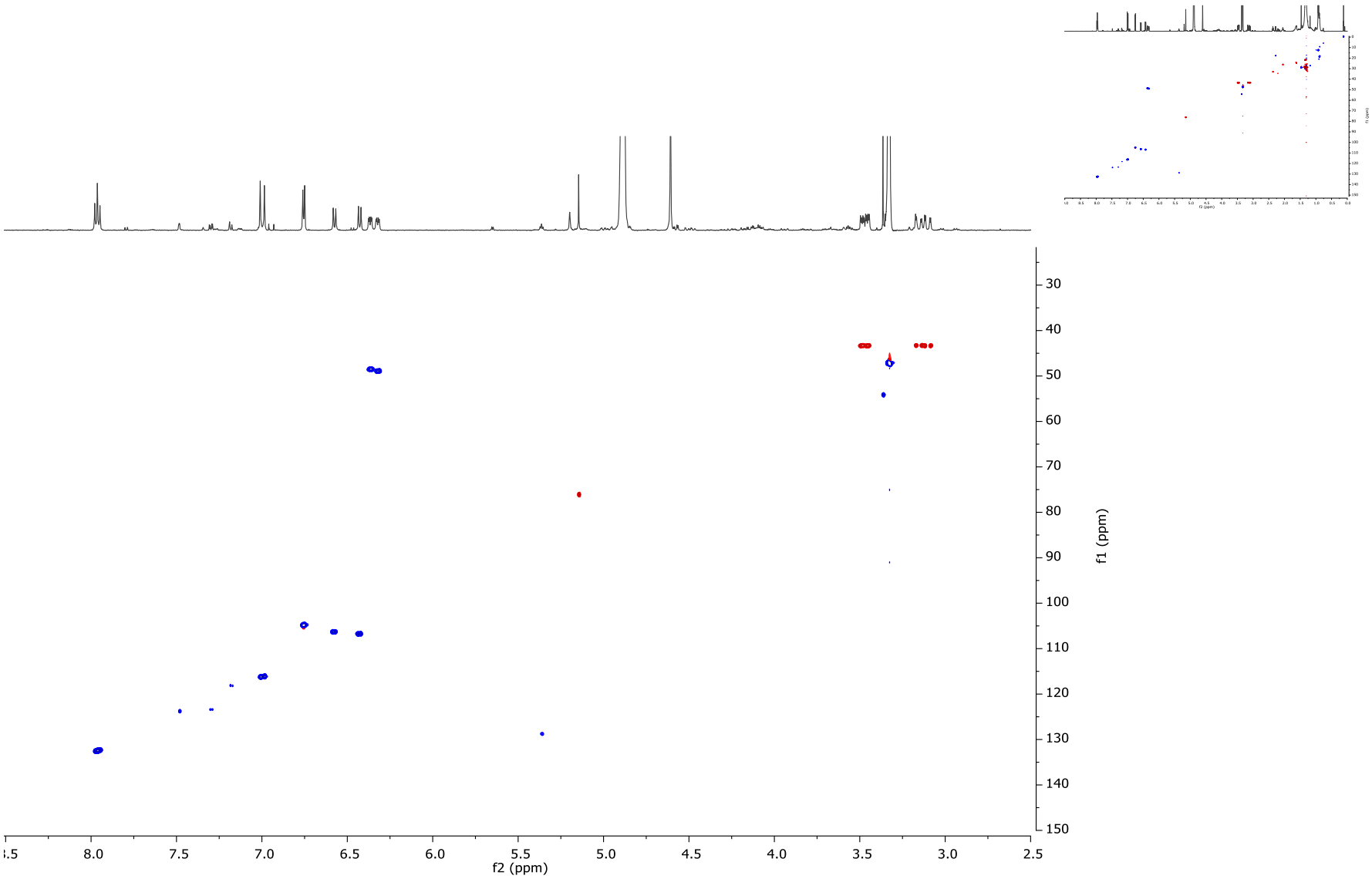

Figure S28. HSQC NMR spectrum of **8** in CD_3OD.

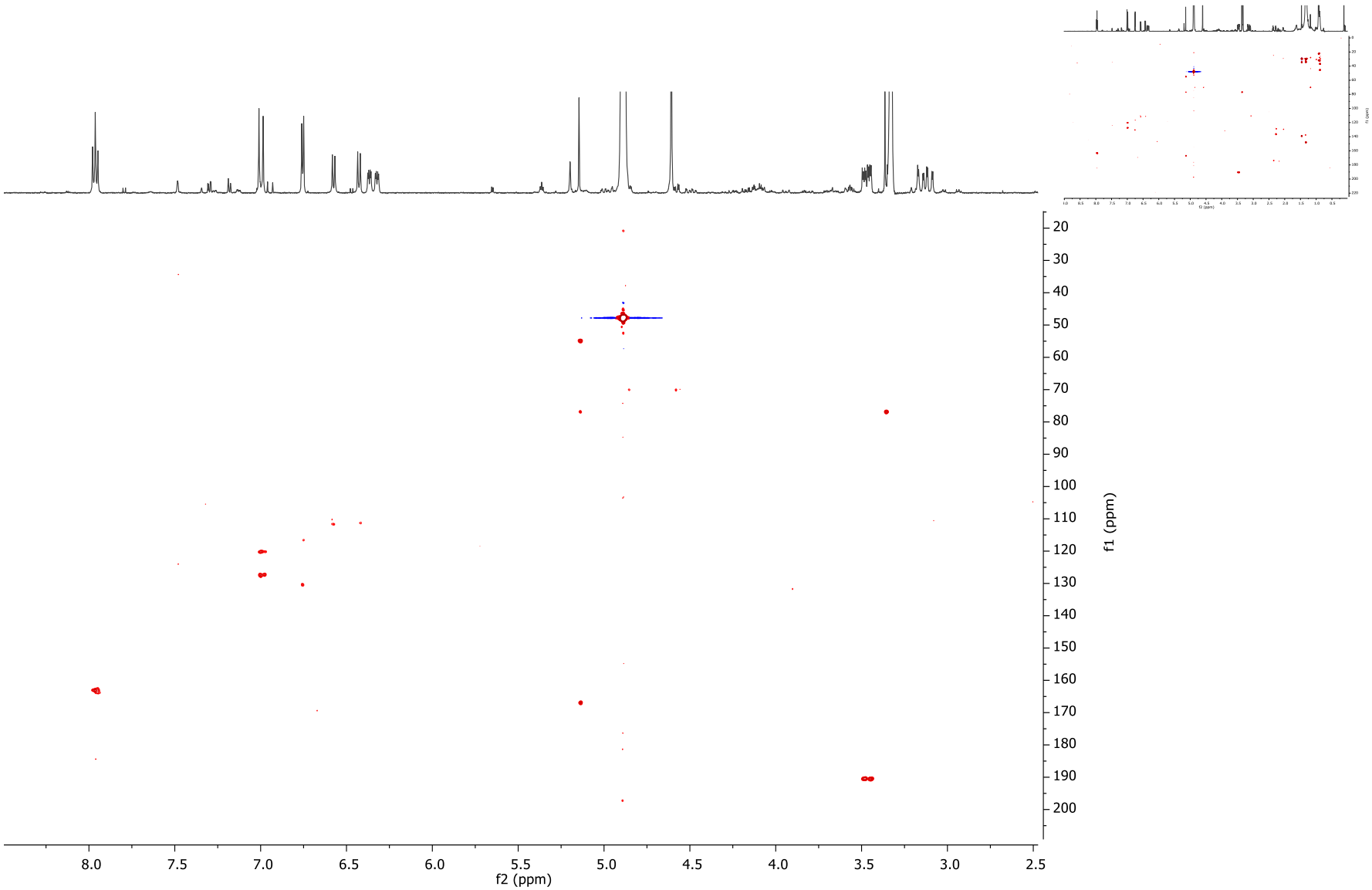

Figure S29. HMBC NMR spectrum of **8** in CD_3OD.

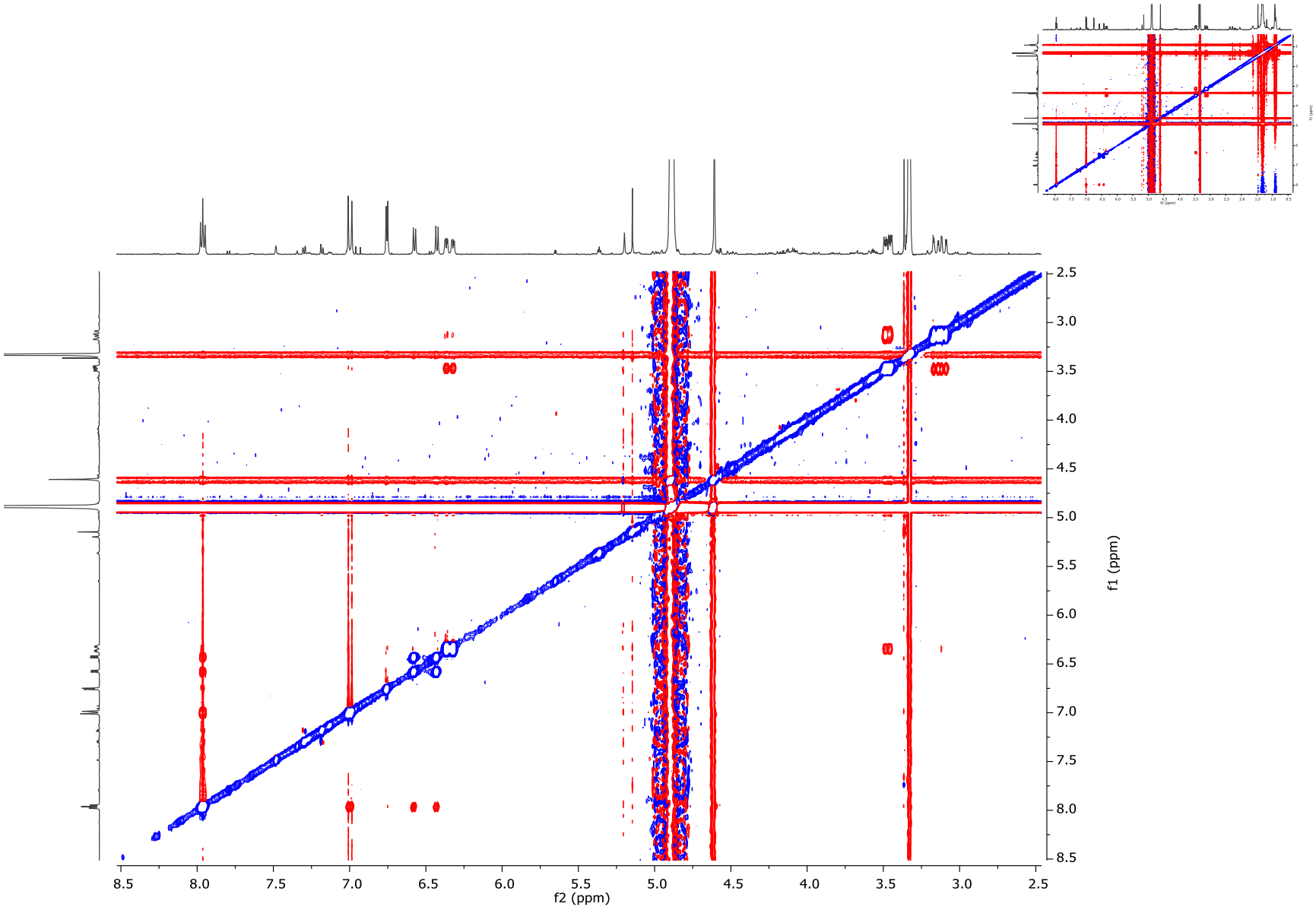

Figure S30. NOESY NMR spectrum of **8** in CD_3OD.

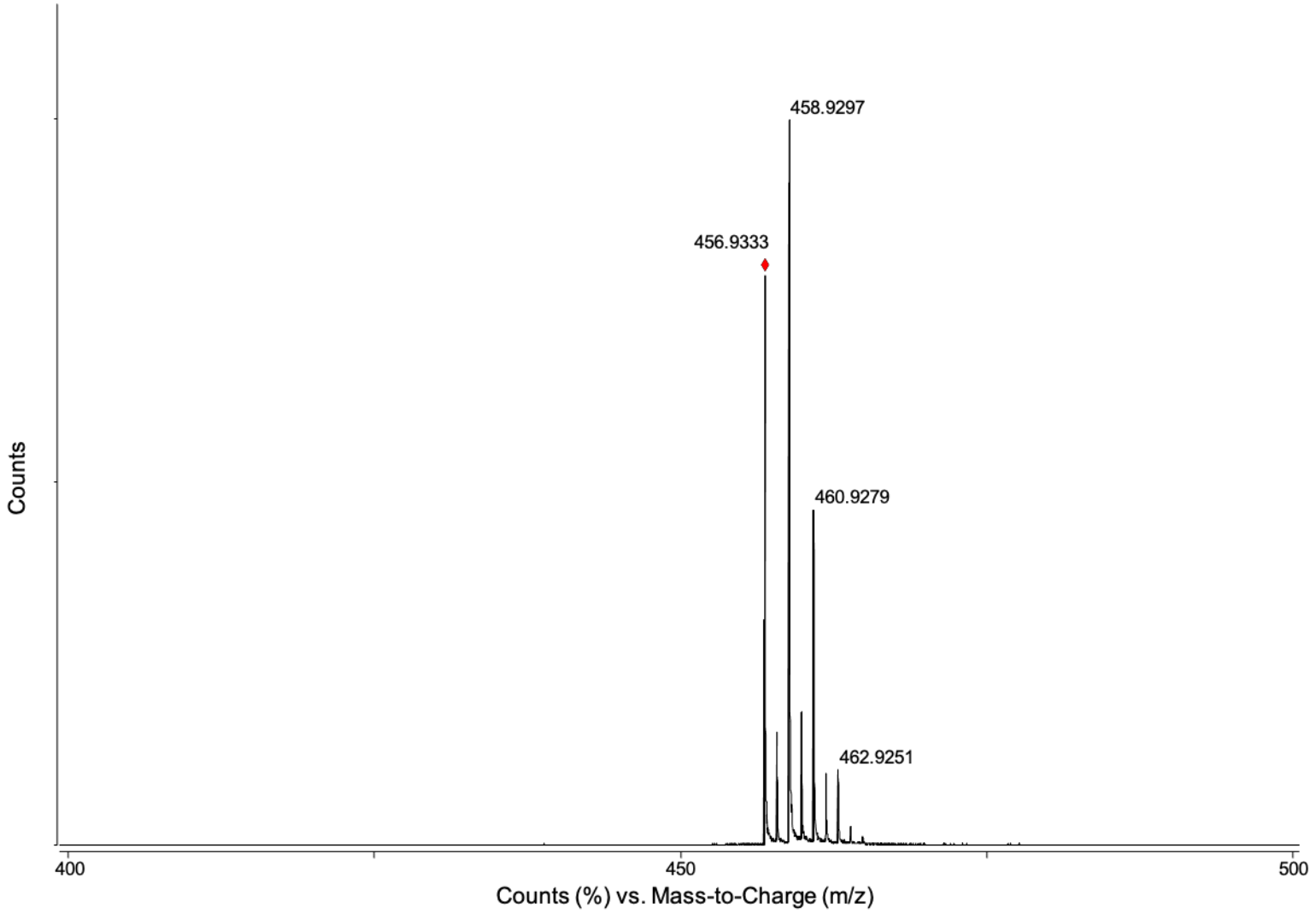

Figure S31. HR-ESI-TOF-MS spectrum of **8**.

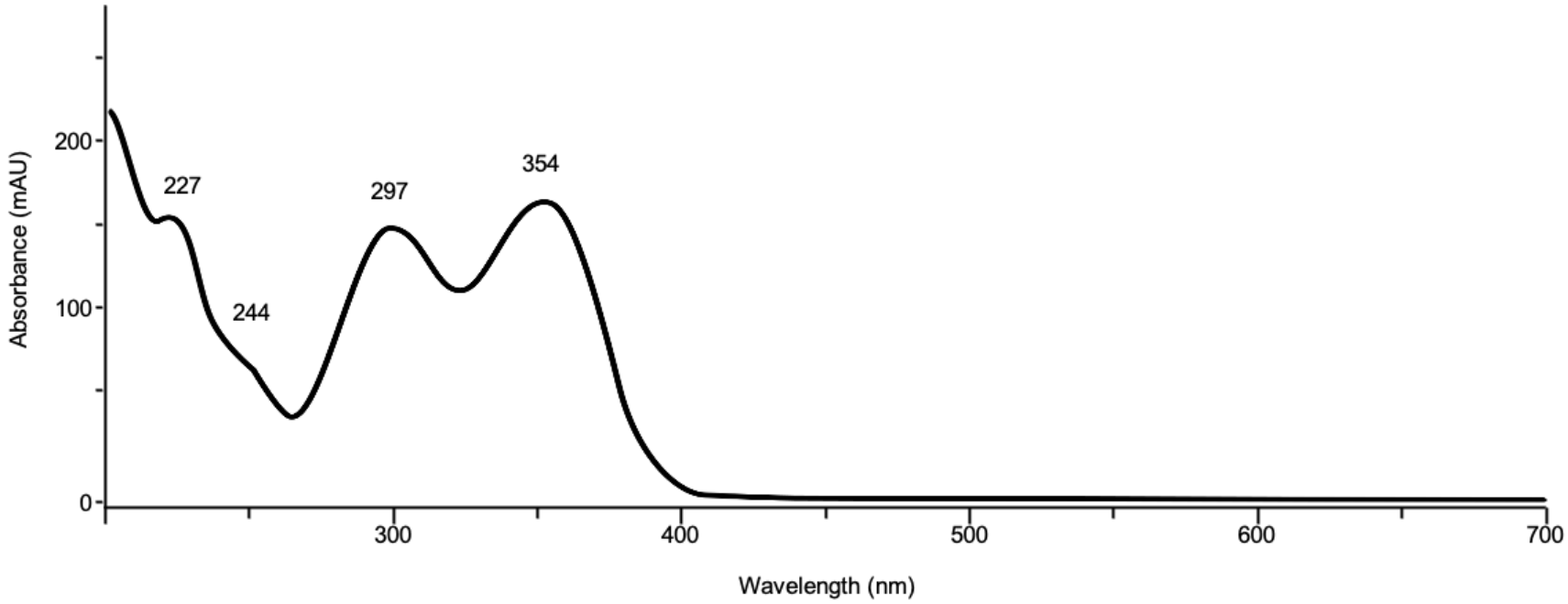

Figure S32. UV/vis spectrum of **8**.

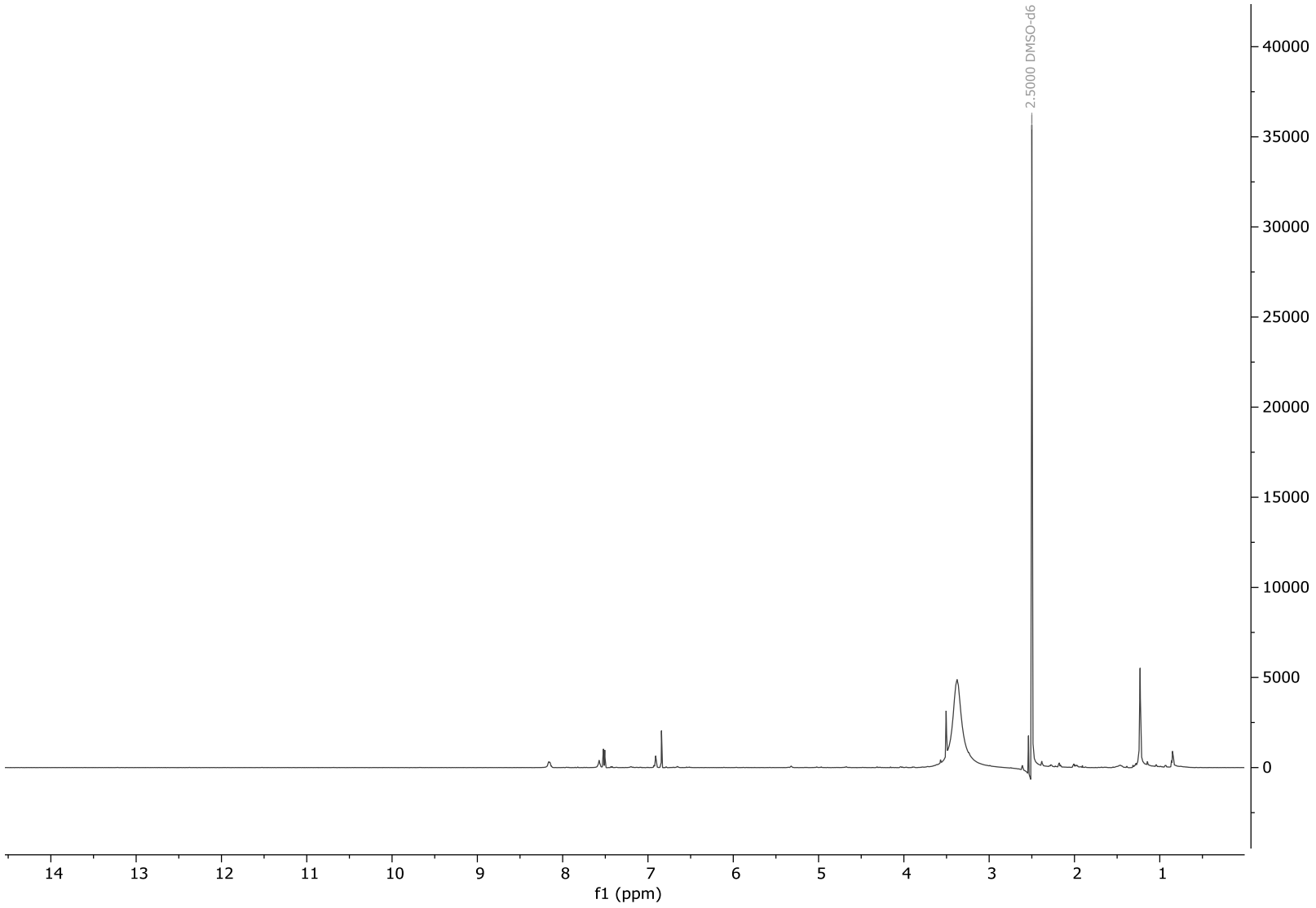

Figure S33. [1]H NMR spectrum of **9/10** after 5 minutes in DMSO-d_6.

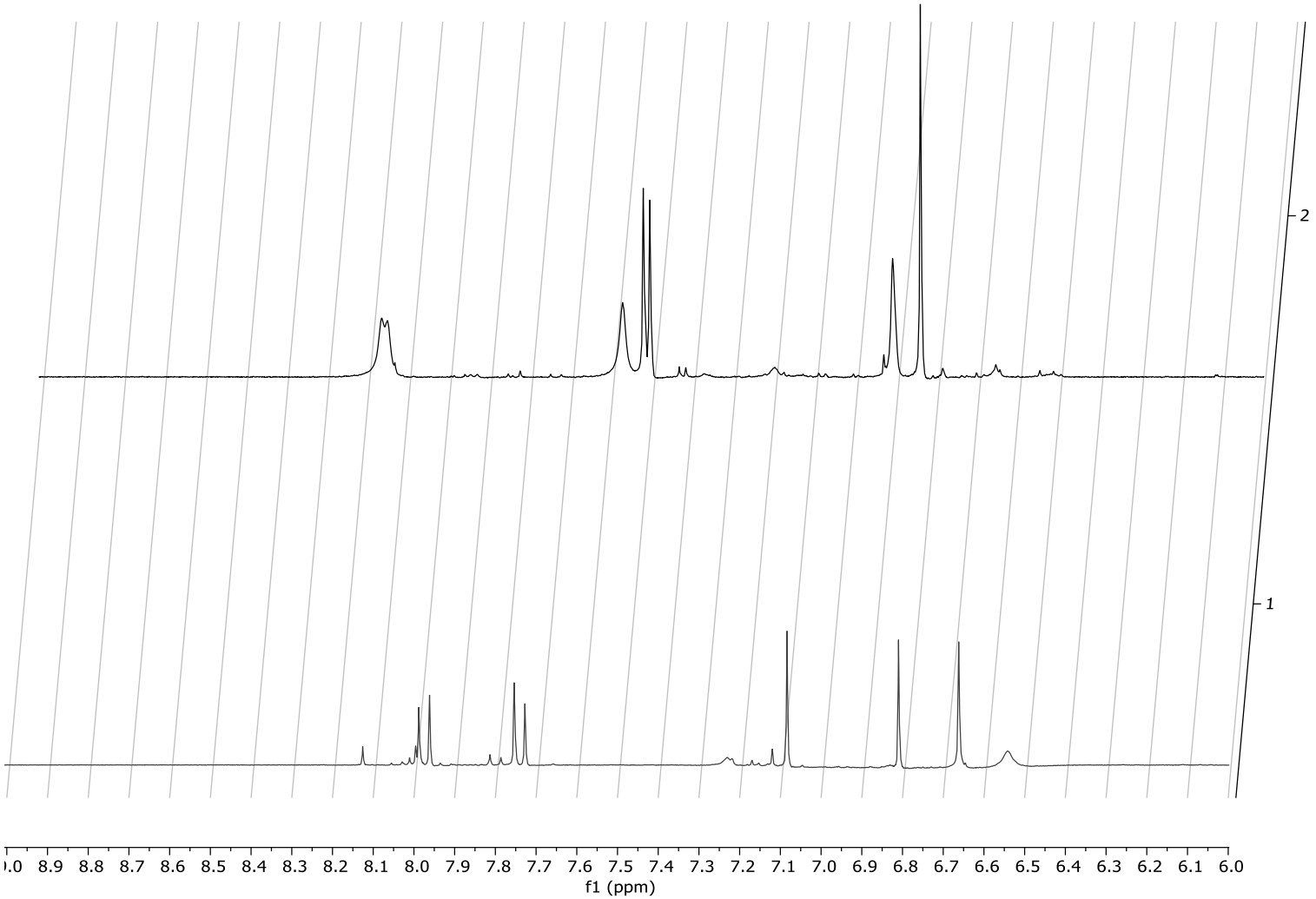

Figure S34. ^{1}H NMR time course comparison of **9** after 5 minutes (top) and 36 hours (bottom) in DMSO-d_6.

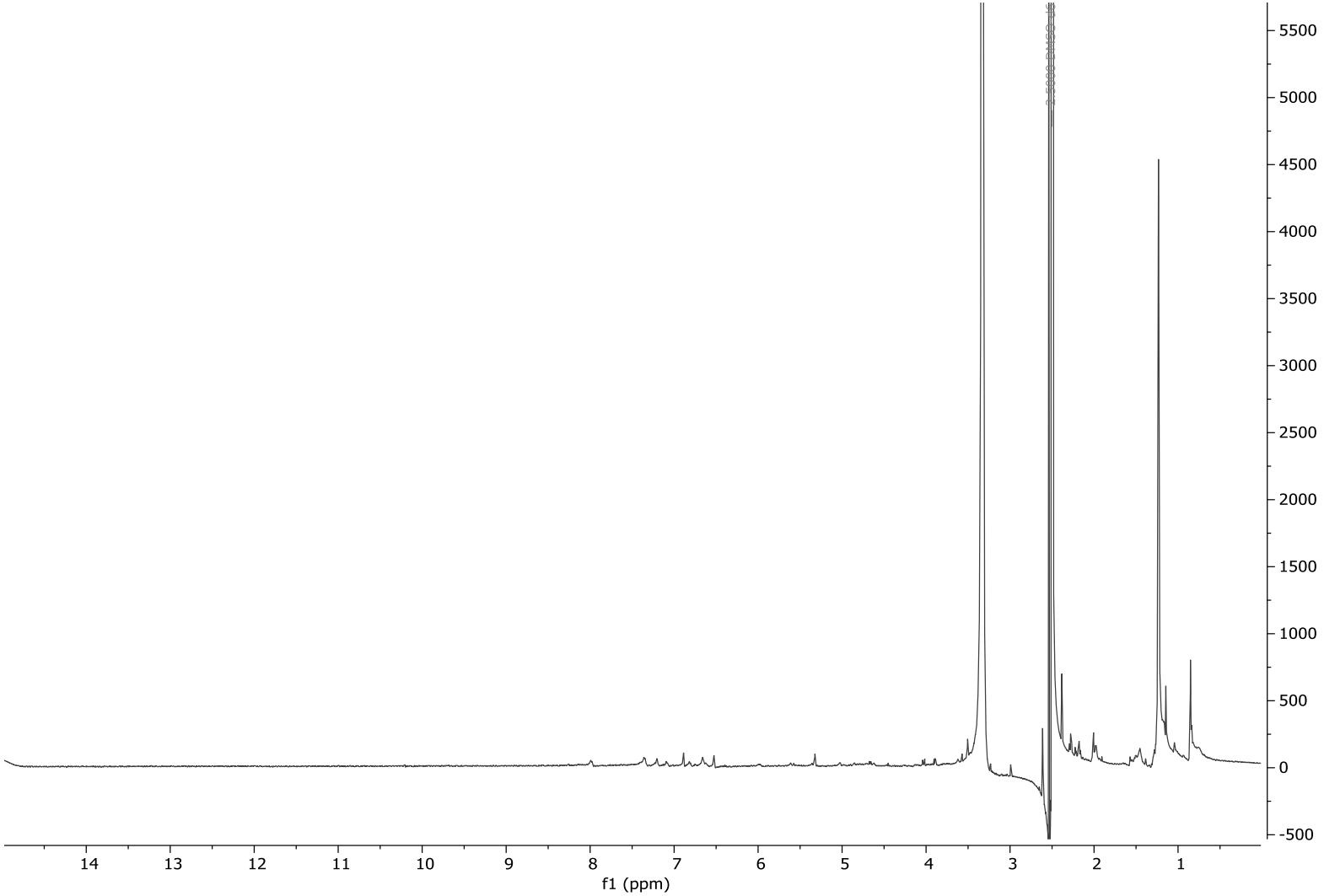

Figure S35. [1]H NMR spectrum of **9/10** after 5 minutes in DMSO-d_6.

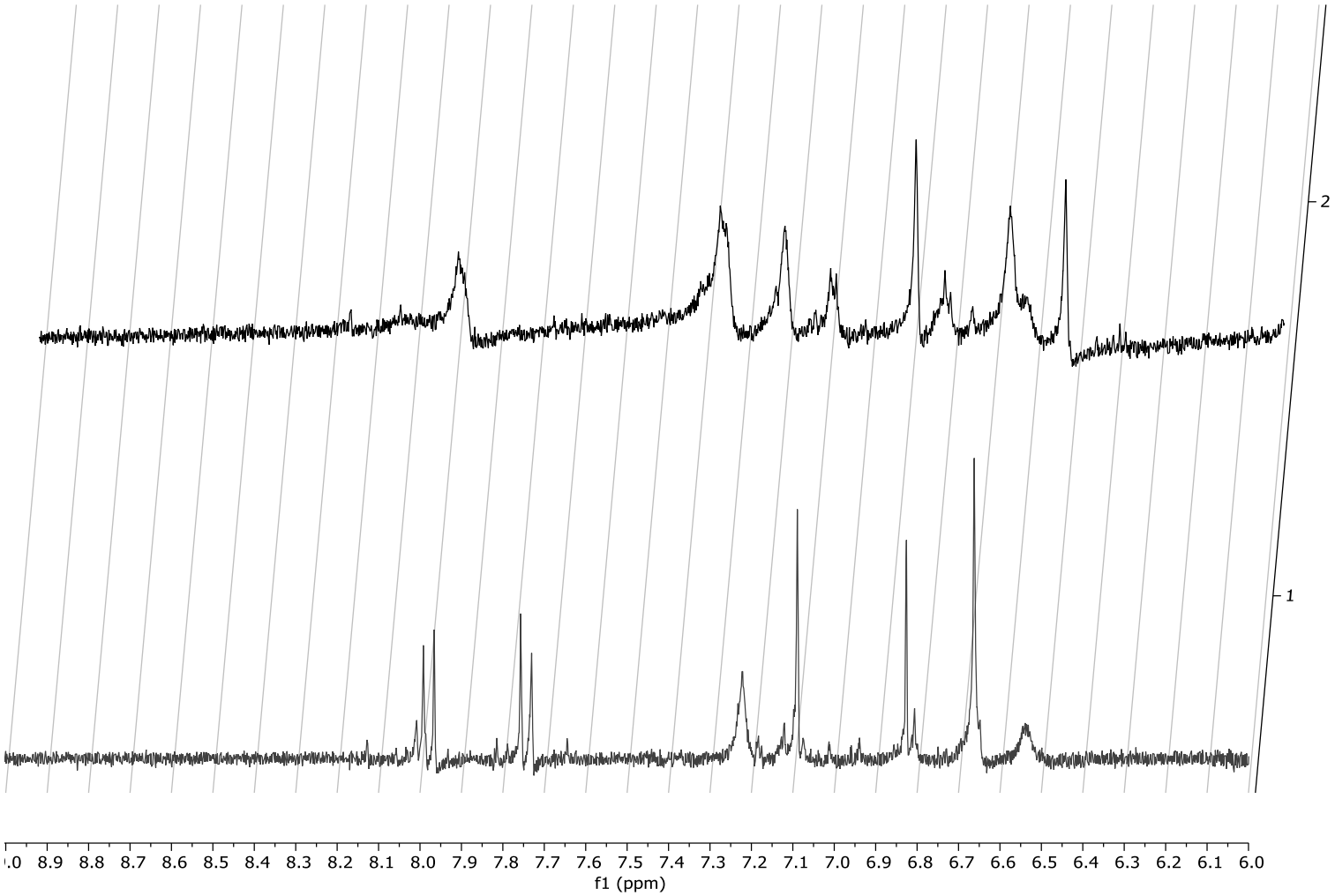

Figure S36. ^{1}H NMR time course comparison of **9/10** after 5 minutes and 36 hours in DMSO-d_6.

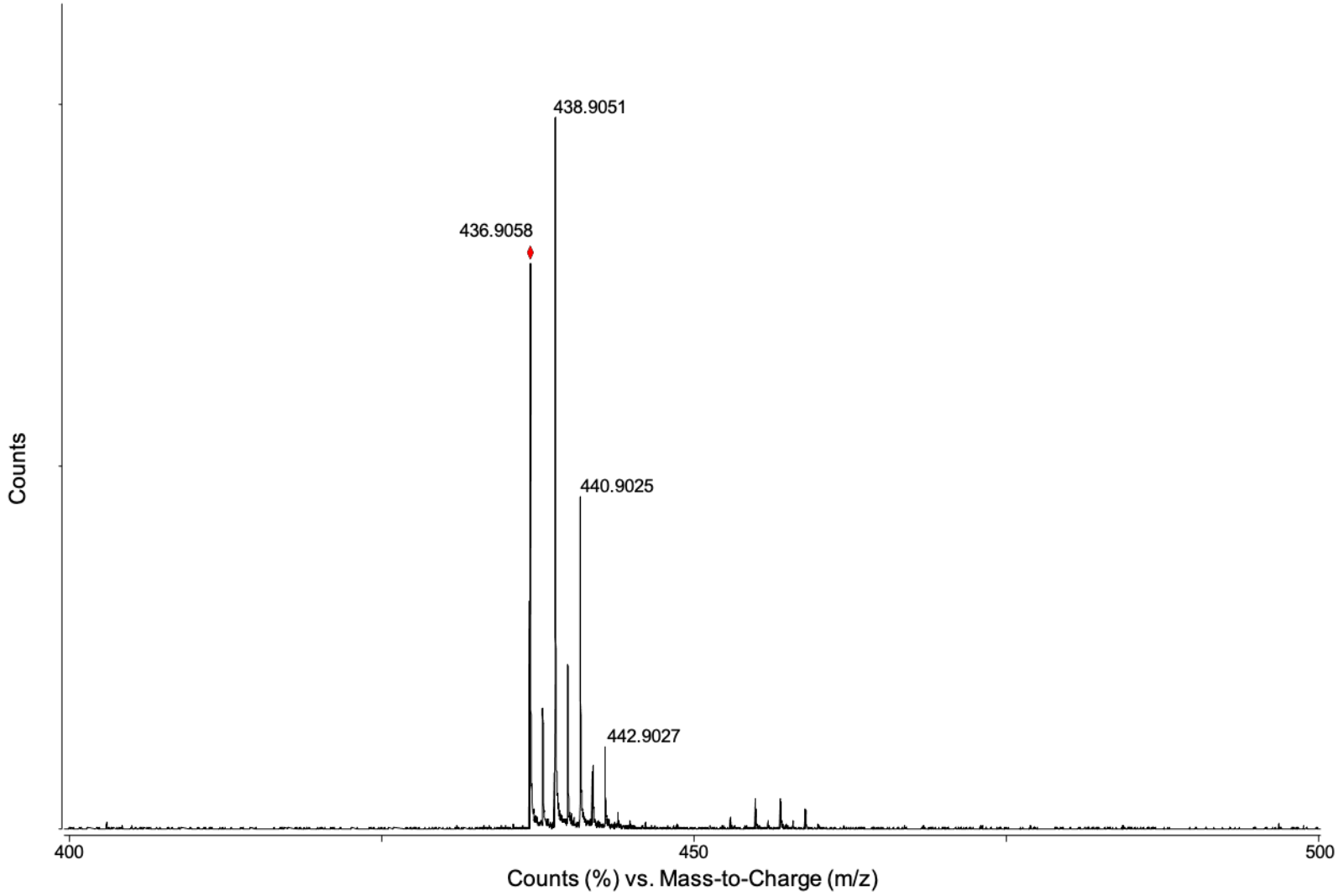

Figure S37. HR-ESI-TOF-MS spectrum of **9/10**.

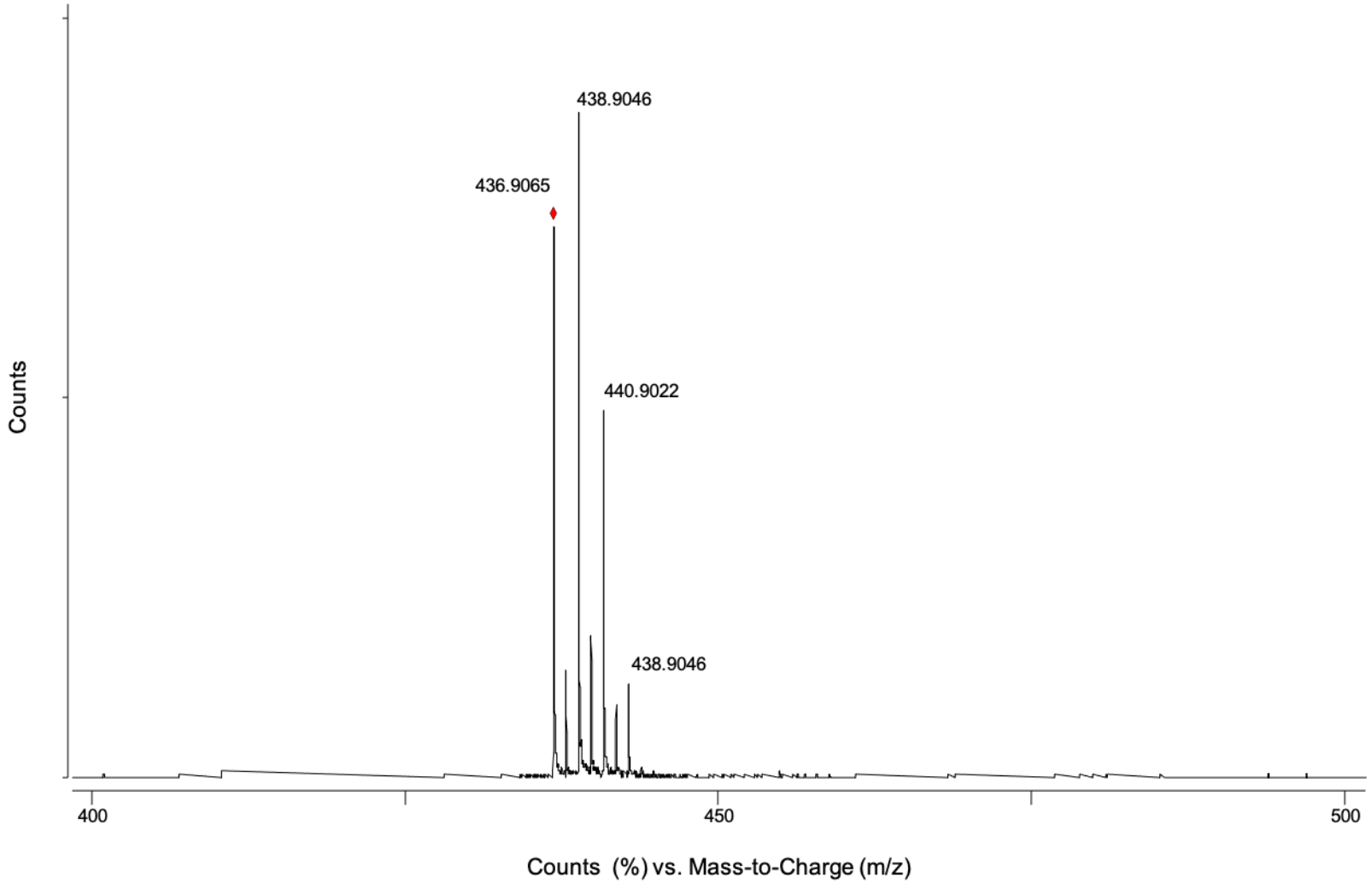

Figure S38. HR-ESI-TOF-MS spectrum of **9/10**.

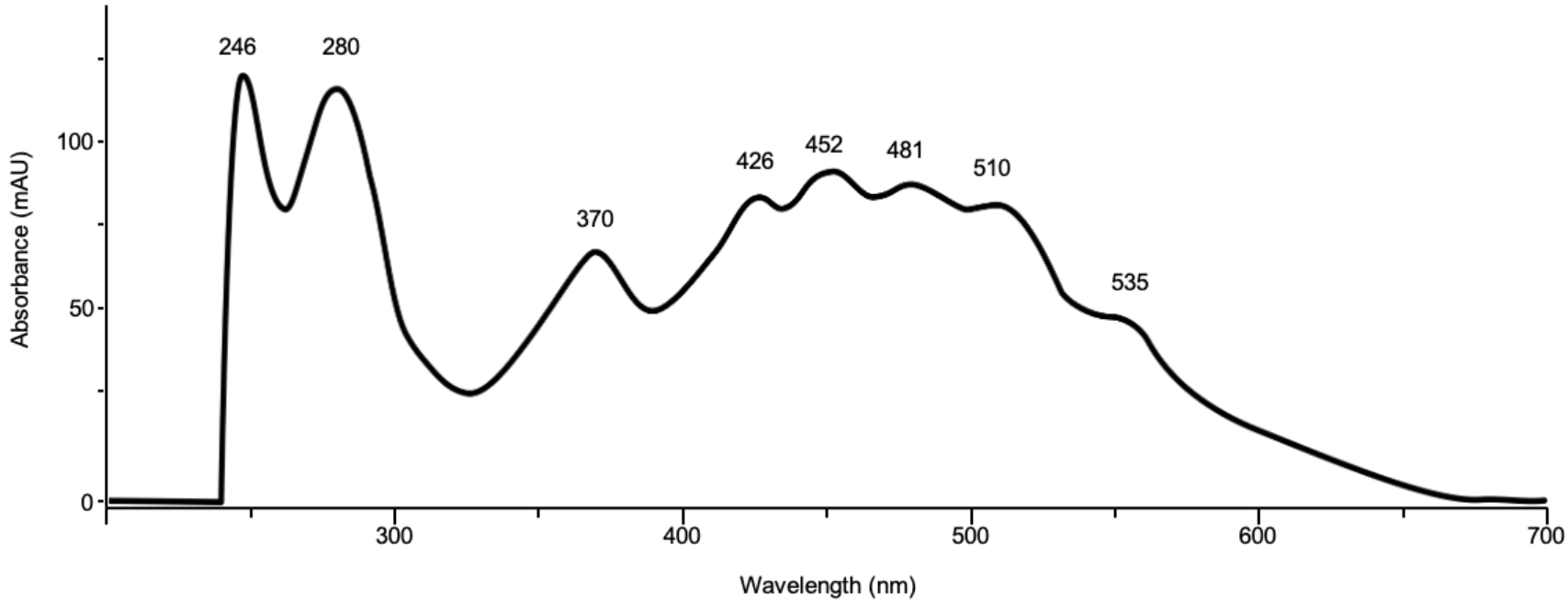

Figure S39. UV/vis spectrum of **9/10** (CH_3OH).

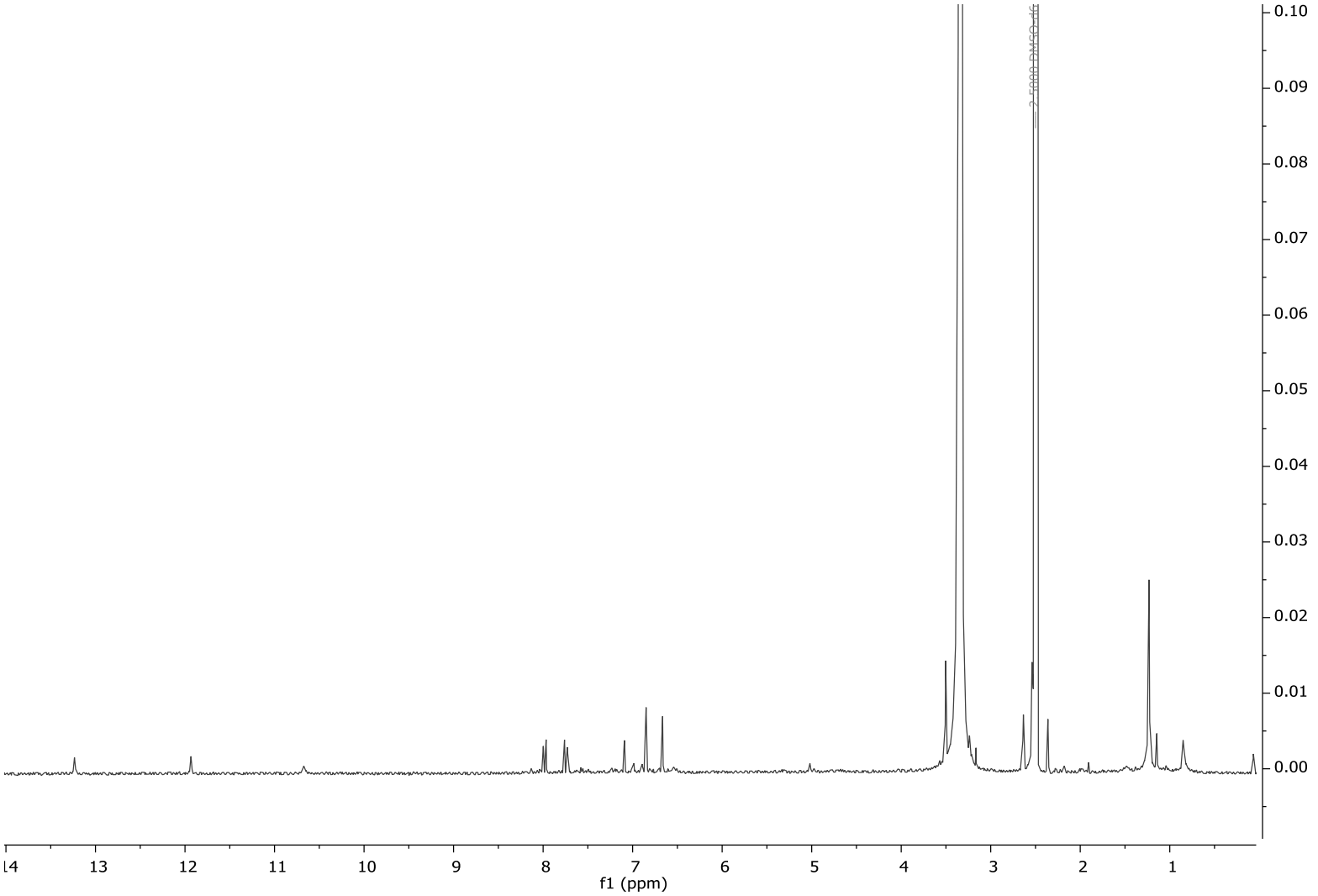

Figure S40. [1]H NMR spectrum of **13** in DMSO-d_6.

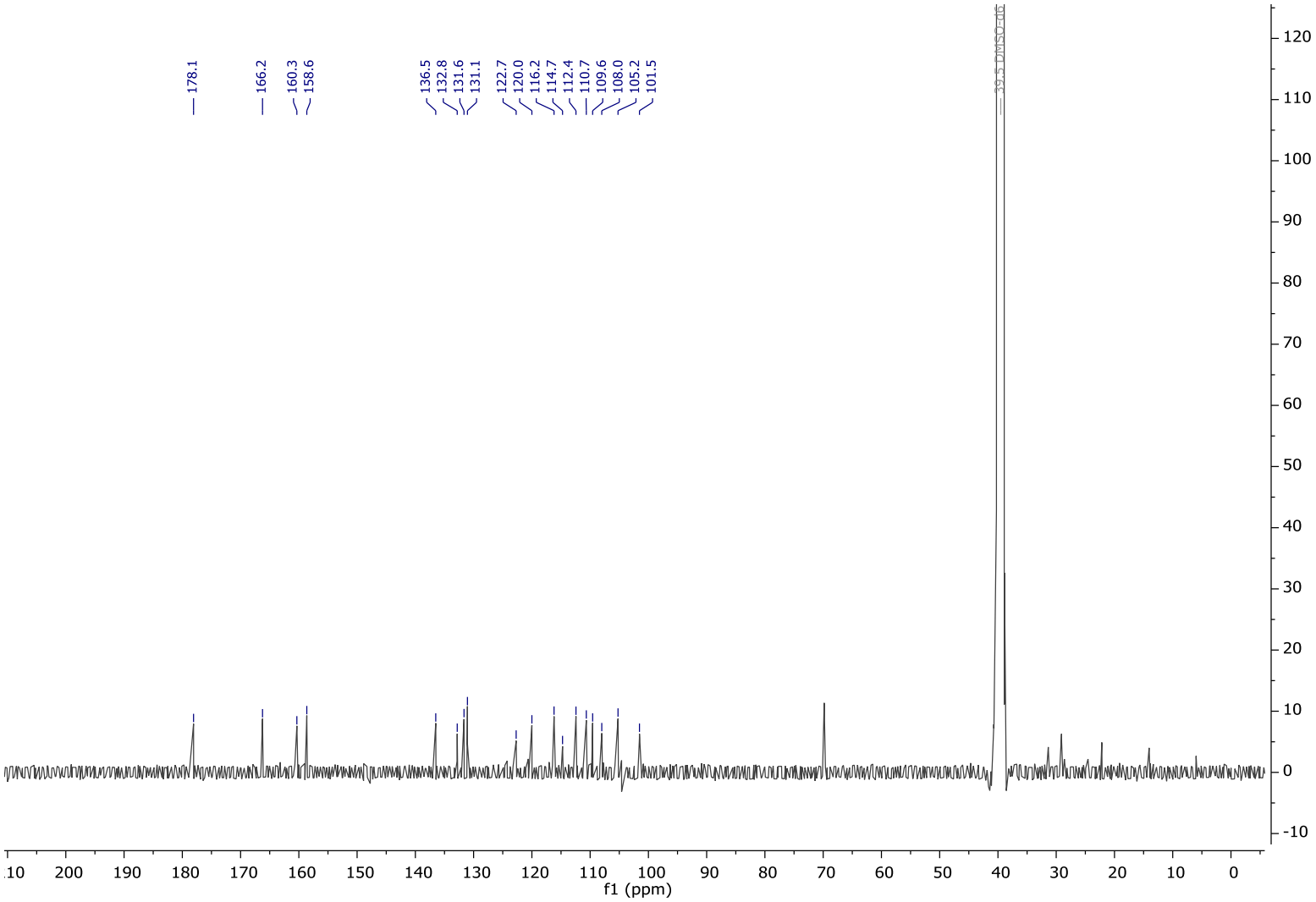

Figure S41. ^{13}C NMR spectrum of **13** in DMSO-d_6.

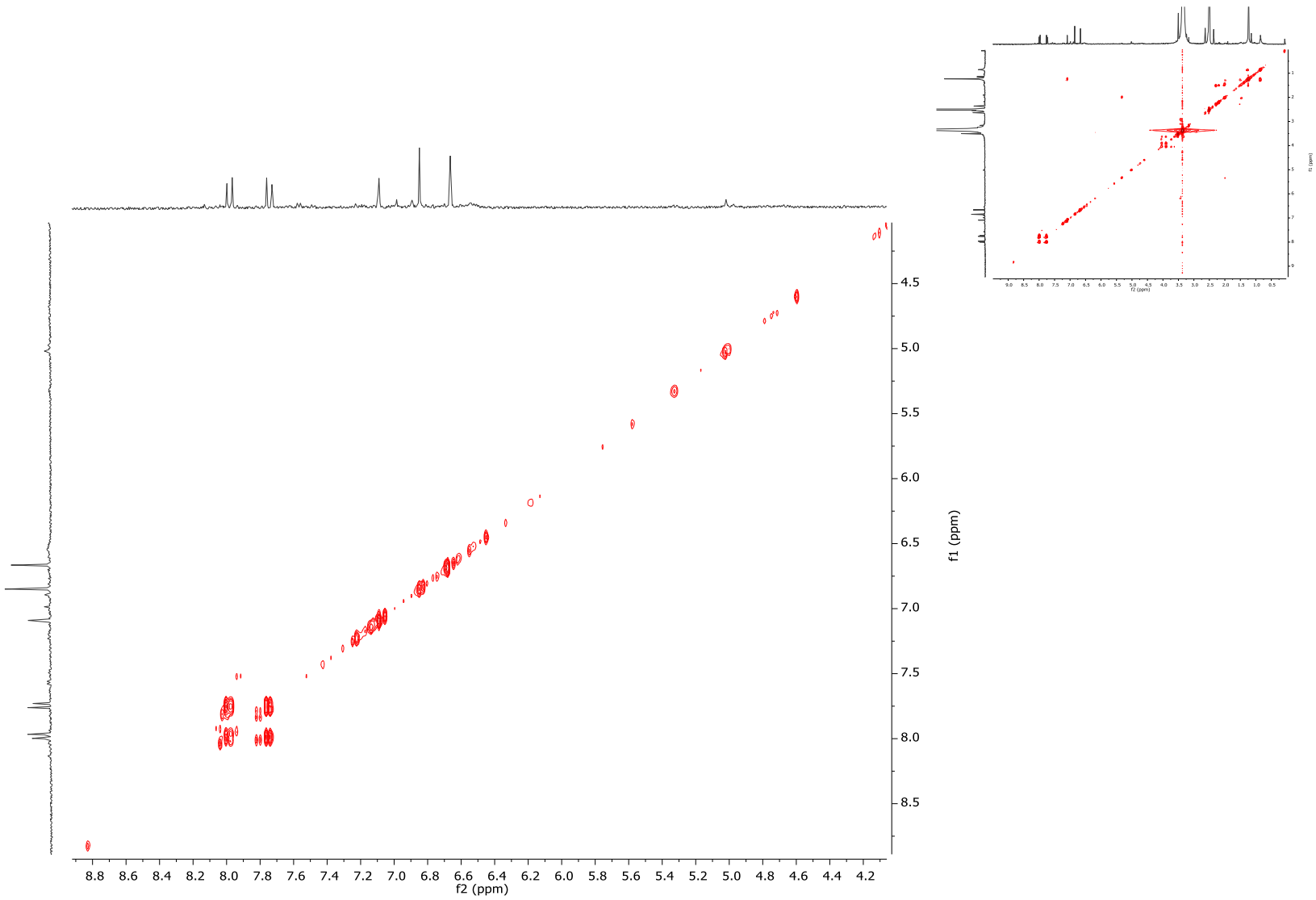

Figure S42. COSY NMR spectrum of **13** in DMSO-d_6.

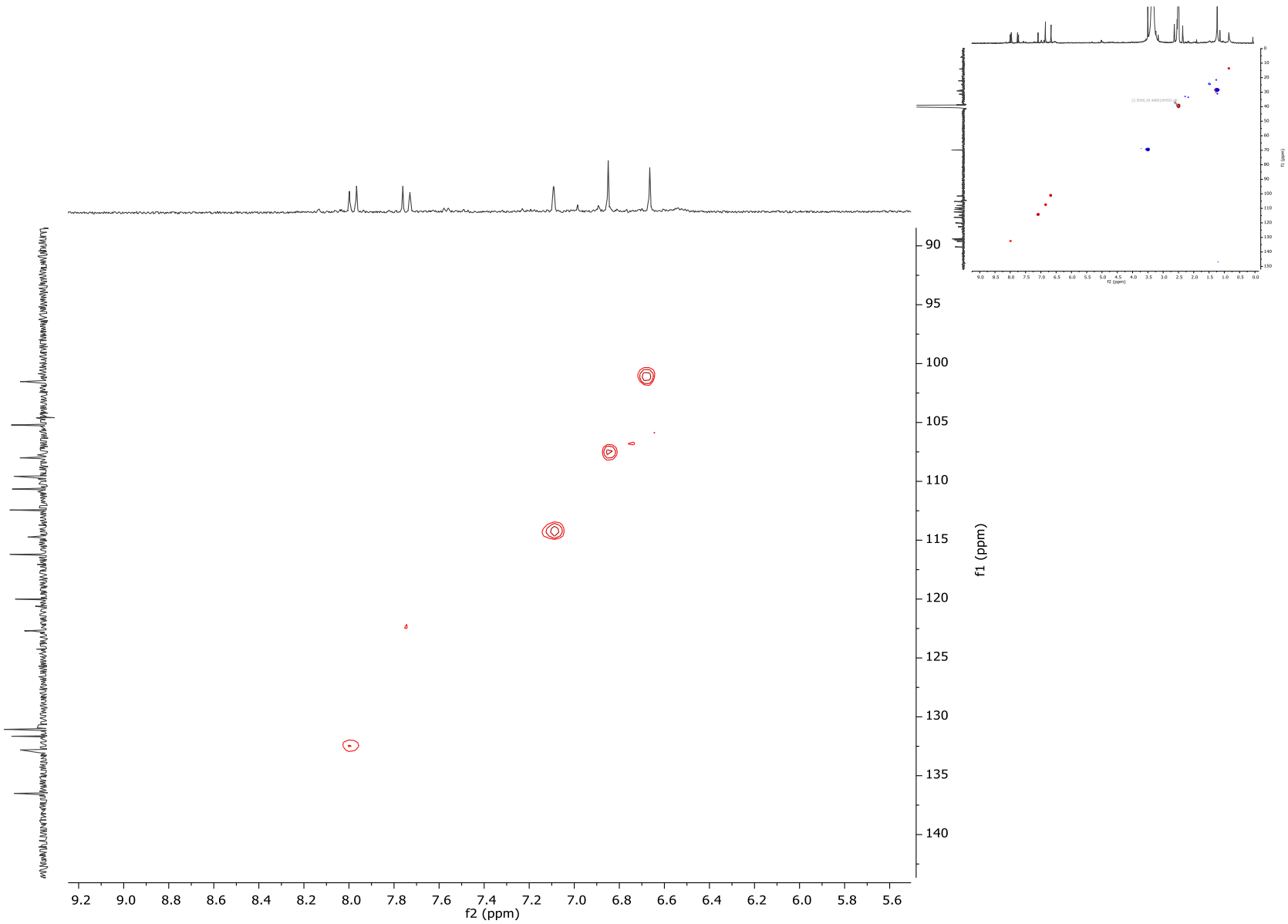

Figure S43. HSQC NMR spectrum of **13** in DMSO-d_6.

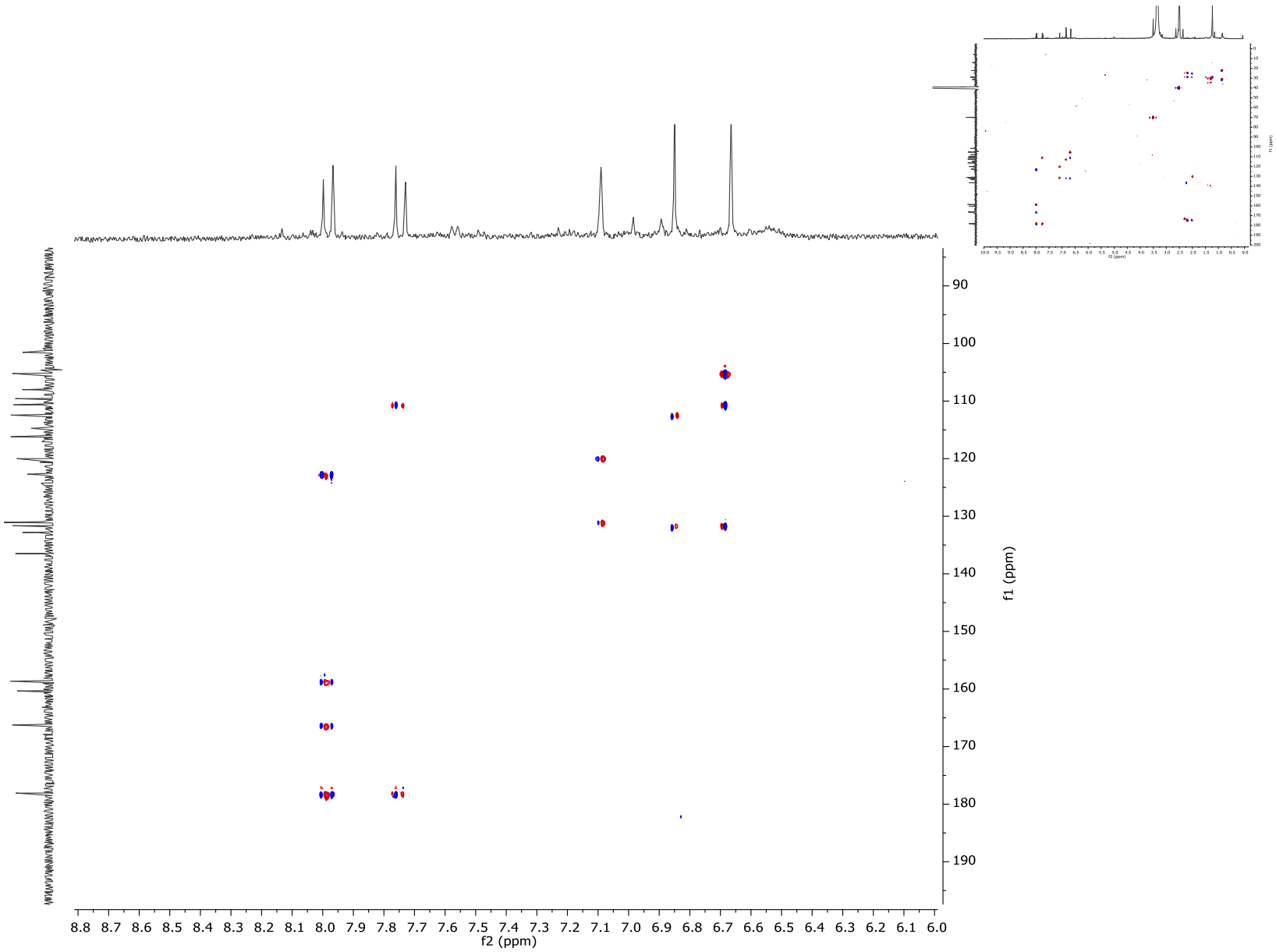

Figure S44. HMBC NMR spectrum of **13** in DMSO-d_6.

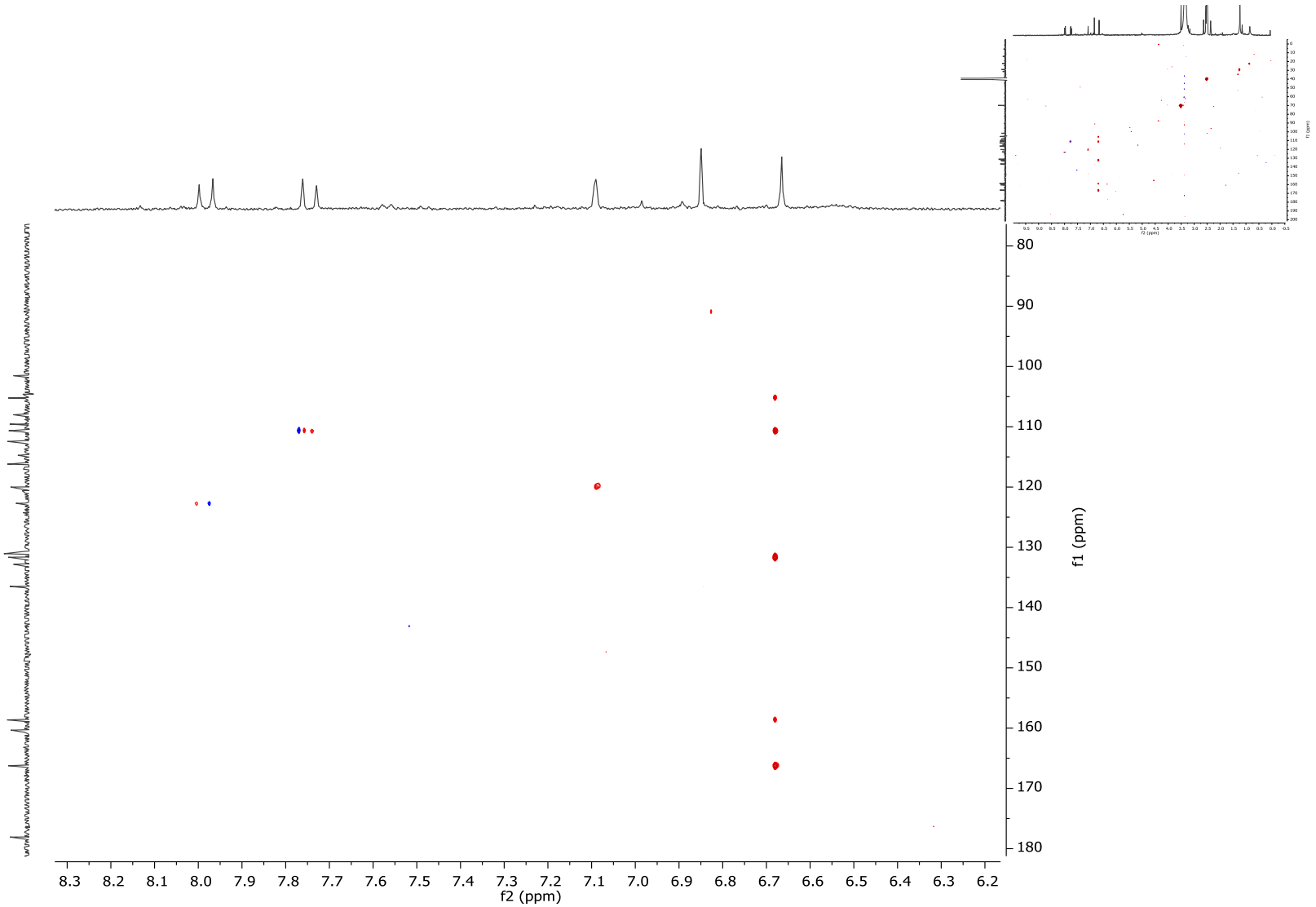

Figure S45. Long-range HMBC NMR spectrum of **13** in DMSO-d_6.

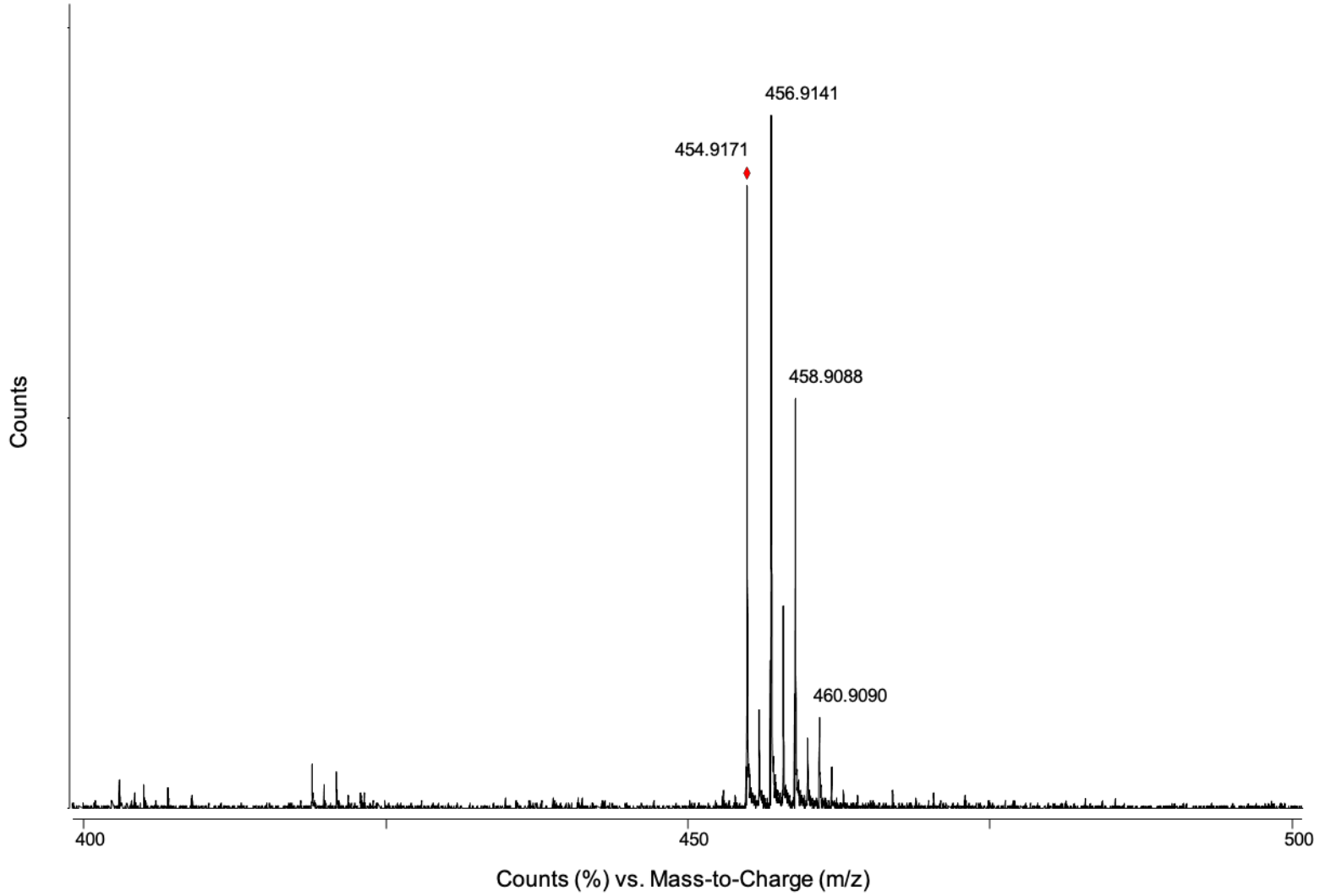

Figure S46. HR-ESI-TOF-MS spectrum of **13**.

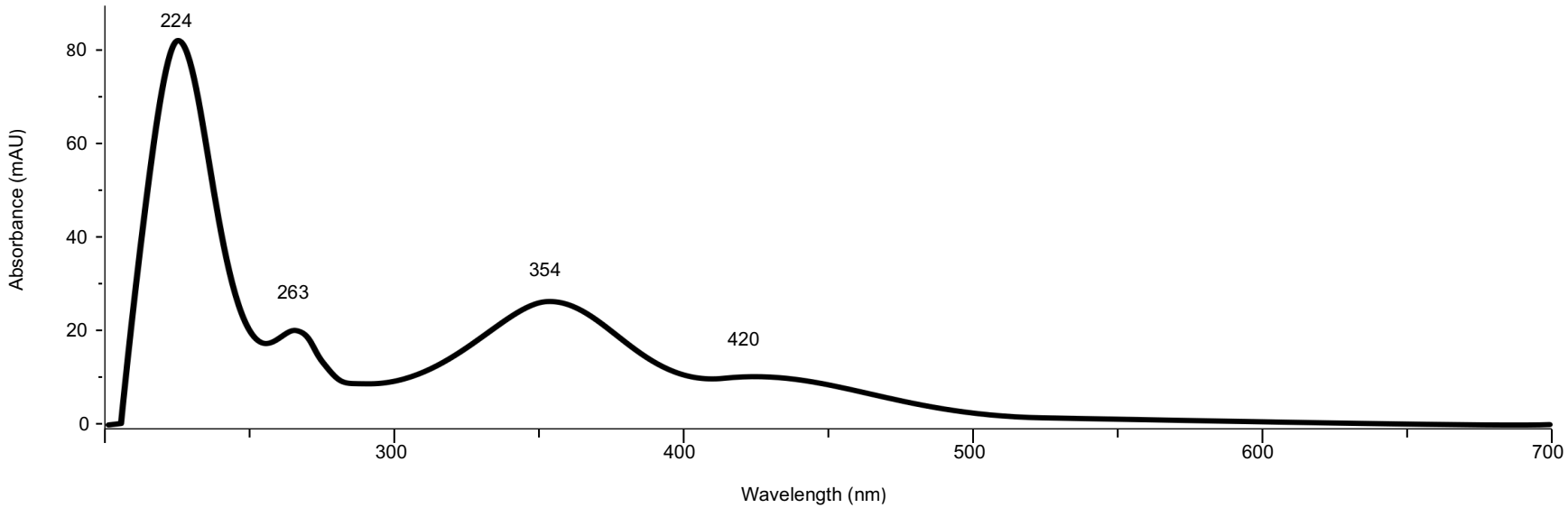

Figure S47. UV/vis spectrum of **13** (CH_3OH).

5. Supplementary References

(1) Kim, M. C.; Cullum, R.; Machado, H.; Smith, A. J.; Yang, I.; Rodvold, J. J.; Fenical, W. *J. Nat. Prod.* **2019**, *82*, 2262–2267.

(2) Mantovani, S. M.; Moore, B. S. *J. Am. Chem. Soc.* **2013**, *135*, 18032–18035.

(3) Kieser, T.; Bibb, M. J.; Buttner, M. J.; Chater, K. F.; Hopwood, D. A. *Practical Streptomyces genetics*; The John Innes Foundation: Norwich, 2000.

(4) Green, M. R.; Sambrook, J. *Cold Spring Harb. Protoc.* **2017**, *2017* (8), 673–674.

(5) Zallot, R.; Oberg, N.; Gerlt, J. A. *Biochemistry* **2019**, *58*, 4169–4182.

(6) Shannon, P.; Markiel, A.; Ozier, O.; Baliga, N. S.; Wang, J. T.; Ramage, D.; Amin, N.; Schwikowski, B.; Ideker, T. *Genome Res.* **2003**, *13*, 2498–2504.

(7) Goujon, M.; McWilliam, H.; Li, W.; Valentin, F.; Squizzato, S.; Paern, J.; Lopez, R. *Nucleic Acids Res.* **2010**, *38*, 695–699.

(8) Mullowney, M. W.; Navarro-Muñoz, J. C.; Selem-Mojica, N.; Kautsar, S. A.; Tryon, J. H.; Parkinson, E. I.; De, E. L. C.; Santos, L.; Yeong, M.; Cruz-Morales, P.; Abubucker, S.; Roeters, A.; Lokhorst, W.; Fernandez-Guerra, A.; Dias Cappelini, L. T.; Goering, A. W.; Thomson, R. J.; Metcalf, W. W.; Kelleher, N. L.; Barona-Gomez, F.; Medema, M. H. *Nat. Chem. Biol.* **2020**, *16*, 60–68.